Transcriptomic Analysis of A Cannabis-Derived Neuroprotective Therapy in a Zebrafish Model of ALS

AUTHORS AND AFFILIATIONS

Ishaan Banwait[1,2], Kelly Boddington[1,3], Eric Soubeyrand[1,3], Jose Casaretto[1,3], Gurkamal Deol[1,4], Akeem Gardner[1*]

[1]Canurta Therapeutics, Mississauga, Canada

[2]University of Waterloo, Waterloo, Canada

[3]University of Guelph, Guelph, Canada

[4]Western University, London, Canada

*Corresponding author: akeem@canurta.com

ABSTRACT

Amyotrophic lateral sclerosis (ALS) is a progressive neurodegenerative disease characterized by motor neuron loss, and currently has limited therapeutic options. To advance the development of effective interventions, we conducted a comprehensive transcriptomic analysis using a zebrafish model of ALS induced by β-N-methylamino-L-alanine (BMAA) exposure. Zebrafish embryos were treated with candidate neuroprotective agents, including CNR-401, Edaravone, and Cannflavin A, and assessed for phenotypic and molecular responses. Leveraging Canurta's DEG

Pipeline Assistant, we performed high-throughput RNA-seq analysis, identifying robust differential gene expression signatures and pathway enrichments associated with both disease and therapeutic intervention. Our results demonstrate that BMAA exposure induces significant motor deficits and widespread transcriptomic alterations, notably upregulating genes involved in neuroinflammation and extracellular matrix (ECM) remodeling. Importantly, treatment with CNR-401 not only produced the most extensive transcriptomic response but also significantly rescued BMAA-induced motor deficits in zebrafish larvae, directly linking molecular changes to phenotypic improvement. Functional enrichment analyses revealed that CNR-401 modulates processes central to ALS pathology, including inflammatory response, ECM organization, calcium signaling, steroid metabolism, and neuronal survival via the PI3K-Akt pathway. Edaravone and Cannflavin A elicited more limited and distinct transcriptomic changes, with Edaravone primarily affecting metabolic and signaling pathways, and Cannflavin A modulating metabolic and steroidogenic functions.

INTRODUCTION

ALS is a rapidly progressive neurodegenerative disease characterized by the loss of motor neurons, leading to muscle weakness, paralysis, and ultimately death. Despite decades of research, effective treatments remain scarce, and the disease burden continues to grow globally. Existing therapies, such as riluzole and edaravone, offer only modest benefits [1], underscoring the urgent need for new therapeutic strategies that target the complex molecular mechanisms underlying ALS pathogenesis.

Zebrafish (*Danio rerio*) provide a powerful vertebrate model for studying neurodegenerative diseases due to their genetic tractability, conserved neurobiology, and suitability for

high-throughput screening. The neurotoxin BMAA is reliably known to induce ALS-like phenotypes in zebrafish, enabling the evaluation of candidate neuroprotective compounds in vivo [2].

Canurta Therapeutics is dedicated to advancing the development of novel ALS therapies through rigorous preclinical research and innovative computational tools. This study presents the first use of the newly developed DEG Pipeline Assistant that facilitates reproducible, high-throughput analysis of RNA-seq data, enabling rapid identification of disease-relevant genes and pathways that help inform therapeutic strategies [3].

BMAA-Treated Zebrafish Model of ALS

To model ALS-like neurodegeneration, we utilized β-methylamino-L-alanine (BMAA), a cyanobacterial neurotoxin known to induce motor neuron toxicity and behavioral deficits in zebrafish [2]. Neurotoxins, and specifically BMAA, are increasingly implicated in ALS pathogenesis [4]. Dietary exposure to BMAA through bioaccumulation in aquatic food webs has been directly linked to ALS clusters, such as the 50-100-fold increase in ALS-parkinsonism-dementia complex observed among the Chamorro people of Guam who show an average of 6.6 μg/g BMAA in their brain tissues [5]. BMAA is thought to cause this neurodegeneration through pathways such as microglial activation, chronic inflammation, and calcium overload [6].

Exposure to BMAA in zebrafish reliably induces ALS-like phenotypes including motor deficits, spinal abnormalities, altered neuromuscular junction morphology, and increased oxidative stress [2], enabling the evaluation of candidate neuroprotective compounds in vivo. Zebrafish share

approximately 70% of their genes with humans, and an estimated 84% of human disease-associated genes have at least one zebrafish ortholog [7], making them a genetically tractable system for modeling human pathologies. Their nervous system exhibits conserved neuroanatomy and neurochemistry, including orthologous cannabinoid receptors (CB1 and CB2) [8], which are critical for evaluating cannabinoid and cannflavin-based therapeutics. Additionally, zebrafish embryos develop rapidly, are optically transparent, and are amenable to high-throughput screening, enabling efficient assessment of neurobehavioral phenotypes and drug efficacy. This approach leverages the genetic, physiological, and pharmacological similarities between zebrafish and humans, providing a robust platform for the preclinical assessment of ALS therapeutics targeting cannabinoid pathways.

CNR-401: A Novel Cannabis-Derived Formulation

CNR-401 represents a strategically assembled combination of bioactive compounds selected for their established neuroprotective and anti-inflammatory properties. This approach leverages the therapeutic potential of phytochemicals derived from *Cannabis sativa* to address pathological changes associated with neurodegenerative conditions. Among other primary cannabinoids, cannabidiol (CBD) serves as the primary active component in this formulation, demonstrating extensive neuroprotective properties through anti-inflammatory and antioxidant effects [9]. CBD has generated significant interest in its therapeutic potential against secondary injury cascades in traumatic brain injuries, which share key pathological characteristics of ALS such as glial cell dysregulation, excitotoxicity, and neuroinflammation [10]. The inclusion of cannabinoid acid precursors further broadens the therapeutic spectrum of CNR-401, as these molecules are known to offer distinct benefits compared to their decarboxylated counterparts [11]. The formulation is also enhanced by select terpene ingredients, which contribute additional anti-inflammatory and

neuroprotective actions [12]. Cannflavin A, a unique prenylated flavonoid, is incorporated due to its exceptional anti-inflammatory properties achieved through dual inhibition of microsomal prostaglandin E2 synthase-1 (mPGES-1) and 5-lipoxygenase (5-LOX) [13], having been found to be ~30 times more effective than aspirin in reducing inflammation [14]. The strategic design of CNR-401 leverages the entourage effect [15,16] in which cannabinoids, terpenes, and flavonoids interact synergistically to amplify overall therapeutic effectiveness. To comprehensively assess its neuroprotective potential in ALS, this study directly compared CNR-401's transcriptomic effects with those of a clinically approved positive control and pure Cannflavin A within the zebrafish model.

MATERIALS AND METHODS

Solvent Toxicity Assessment

Solubilizers were necessary to make cannabinoids and terpenes in the test formulations miscible in water, as these compounds are inherently not water-soluble, creating challenges for aquatic organism testing. Two cyclodextrin solubilizers were evaluated: hydroxypropyl-β-cyclodextrin (HPC) and hydroxyethyl-β-cyclodextrin (HEC). Cyclodextrins are cyclic oligosaccharides that act as solubilizing agents and are utilized in many commercially available drugs.

For each cyclodextrin, 100 mM stock solutions in water were prepared. Toxicity assays for both cyclodextrins were completed at 6 days post-treatment and performed at concentrations of 0, 0.5, 1, 5, 10, and 20 mM. Following positive results with HEC, extended toxicity testing was conducted with concentrations of 0, 15, 20, 30, 40, and 50 mM using a freshly prepared stock solution. Based on these results, all subsequent experiments were performed using 10 mM HEC

as the final concentration to maintain safety margins while accounting for potential additive toxicity from test compounds.

Product Toxicity Assessment

Toxicity assessments were performed on CNR-401 and Cannflavin A at final concentrations of 0, 0.5, 1, 2, 5, and 10 µM. CNR-401 concentrations were expressed in terms of the highest concentration principal active component (CBD) of the complex botanical mixture. Cannflavin A was used as a reference standard. All toxicity assays were completed at 6 days post-treatment with HEC maintained at 10 mM final concentration in all conditions. Diluted solutions were prepared in HEC 5-10 minutes before addition to multi-well plates.

Product Efficacy Assessment and Phenotypic Analysis

At 8 hours post-fertilization, zebrafish embryos were distributed into 48-well plates (1 per well) and exposed to BMAA at optimized concentrations to induce ALS-like neurodegeneration. Test compounds (CNR-401 and Cannflavin A) were administered simultaneously at their respective NOTEC concentrations. Each experimental plate contained non-treated controls, BMAA-treated controls, and BMAA + compound-treated wells (8 wells per condition). Edaravone, the currently available ALS medication, was included as a positive control. Plates were incubated at 28°C throughout the experimental period.

Behavioral assessments were conducted using the DanioVision automated behavioral tracking system [17] equipped with a GigE camera. At 6 days post-fertilization, zebrafish larvae were placed in the DanioVision system and exposed to white light (15–16 µM/s/m) for 1 minute, followed by tracking for 20 minutes under light conditions. Locomotion patterns were recorded

and analyzed using EthoVision XT17 software [17] to generate comprehensive behavioral profiles. Following behavioral recording, larvae were visually examined to assess phenotypic responses and remove any dead, necrotic, or morphologically affected specimens from the analysis. Visual assessments included evaluation of cardiac edema, abnormal heart rate, body deformation, and overall morphological integrity. Only larvae displaying normal morphology and survival were included in the final behavioral analysis to ensure data quality and experimental validity. Distance moved (mm) served as the primary behavioral endpoint, with BMAA treatment expected to significantly reduce locomotion compared to untreated controls. Effective neuroprotective compounds were anticipated to demonstrate rescue effects by restoring locomotor activity toward control levels.

Experimental Conditions and Replication

To investigate transcriptomic responses to neuroprotective therapies in a zebrafish model of ALS, we designed a multi-condition experiment utilizing six biological replicates per group. Zebrafish embryos were randomly assigned to one of five experimental conditions:

- Control: Untreated zebrafish embryos, serving as the baseline reference
- BMAA: Embryos exposed to β-N-methylamino-L-alanine to induce neurodegenerative phenotypes characteristic of ALS
- CNR-401: BMAA-exposed embryos subsequently treated with Canurta's drug candidate CNR-401
- Edaravone: BMAA-exposed embryos subsequently treated with edaravone, a clinically approved ALS therapy
- Cannflavin A: BMAA-exposed embryos subsequently treated with cannflavin A

Sample Preparation and RNA Sequencing

Non-control zebrafish embryos were exposed to BMAA to induce neurodegeneration, with additional groups receiving candidate neuroprotective agents, including edaravone and CNR-401. RNA was extracted using the Qiagen RNeasy kit and libraries were prepared with the Illumina TruSeq Stranded RNA kit. Sequencing was performed on an Illumina NovaSeq 6000 platform, yielding an average of 36.3 million read pairs per sample.

Data Processing and Visualization

Raw reads were trimmed with cutadapt [18] and mapped to the Danio rerio reference genome using STAR [19,20]. Fastqc [21] was used to analyze the quality of the reads before and after trimming. Gene-level counts were subsequently imported into DESeq2 [22] for normalization and pairwise differential expression analysis. Lastly, the Canurta DEG Pipeline Assistant [3] was employed for downstream analysis:

- Automated metadata construction and quality control (boxplots, correlation heatmap, PCA)
- Differential expression filtering with log2 fold change > 1 and adjusted p-value < 0.05
- Visualization (MA plots, volcano plots, heatmaps)
- Ortholog mapping to human genes
- GO and KEGG functional enrichment analysis with adjusted p-value < 0.05

(Supplementary Material: Screenshot of DEG Pipeline Assistant Parameters Used).

RESULTS

Solvent Toxicity Assessment

HPC demonstrated significant toxicity at 5 mM concentration, resulting in 75% larval mortality with observable toxicity in surviving larvae including cardiac edema, abnormal heart rate, and body deformation. Complete mortality was observed at 10 mM and 20 mM concentrations. In contrast, HEC showed no toxicity up to 20 mM, with all larvae surviving and displaying no morphological changes or significant decrease in movement.

Product Toxicity Assessment

Both CNR-401 and Cannflavin A demonstrated no toxicity up to 2 µM concentration (Supplementary Material: Product Toxicity Assays). CNR-401 showed 62.5% larval survival at 5 µM and complete mortality at 10 µM, yielding an LC50 of 4.827 µM. Cannflavin A exhibited 37.5% survival at 5 µM and complete mortality at 10 µM, with an LC50 of 4.694 µM. Teratotoxicity assessments closely followed acute toxicity trends for both compounds.

Given that both products were safe up to a final concentration of 2 µM, the assays were repeated in three biological experiments in order to explore the toxicity between 2 and 5 µM to find the maximum safe concentrations.

Product Efficacy Assessment

BMAA treatment significantly reduced locomotion in zebrafish larvae ($p < 0.0001$), confirming the validity of the neurodegeneration model. Edaravone, the current ALS medication, demonstrated significant rescue effects ($p = 0.0002$) on BMAA-treated larvae mobility. Both CNR-401 and Cannflavin A showed significant rescue effects with p-values of $p < 0.0001$ and p

= 0.0054, respectively (Figure 1). All treatments were administered at 2 µM concentration with nine biological replicates per condition.

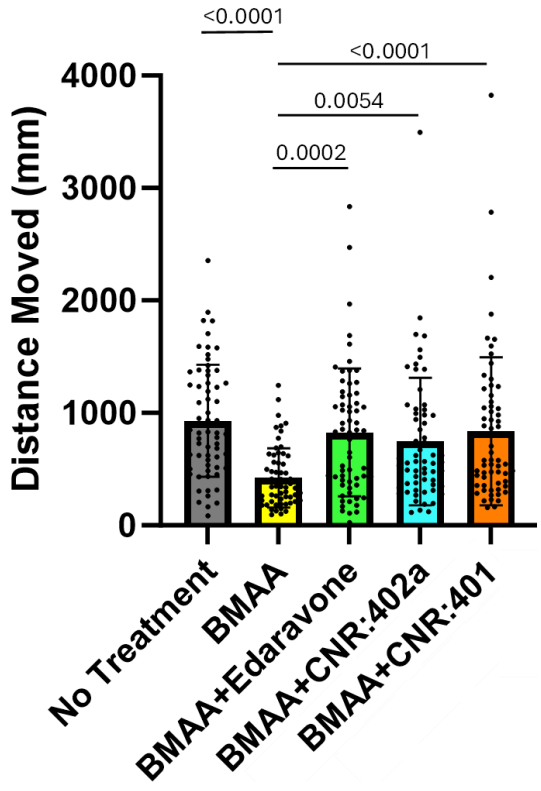

Figure 1. Effect of CNR-401 and Cannflavin A (CNR-402a) in a BMAA-induced model of neurotoxicity in zebrafish larvae. All treatments are dosed at 2 µM. Experiments were done with nine biological replicates.

Product Dose-Response Analysis

CNR-401 demonstrated dose-dependent efficacy with the lowest effective dose of 0.5 µM in the BMAA-induced neurotoxicity model (Figure 2). Cannflavin A required a higher concentration, showing efficacy beginning at 1 µM (Figure 3). This difference indicates superior potency for

CNR-401 at lower concentrations. Seven biological replicates were completed for each condition in the dose-response studies.

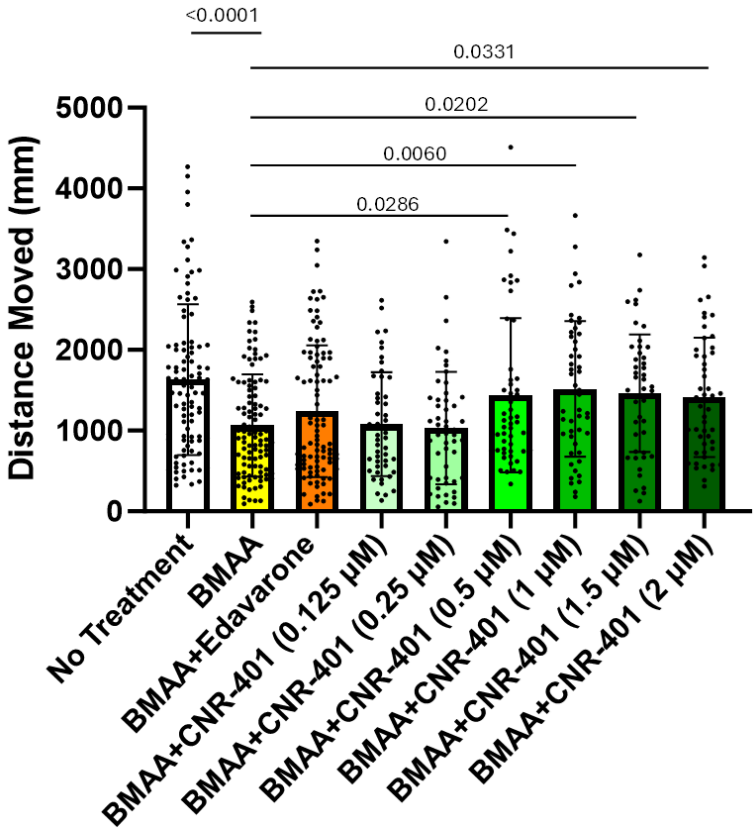

Figure 2. Dose response of CNR-401 in a BMAA-induced model of neurotoxicity in zebrafish larvae. Experiments were done with seven biological replicates.

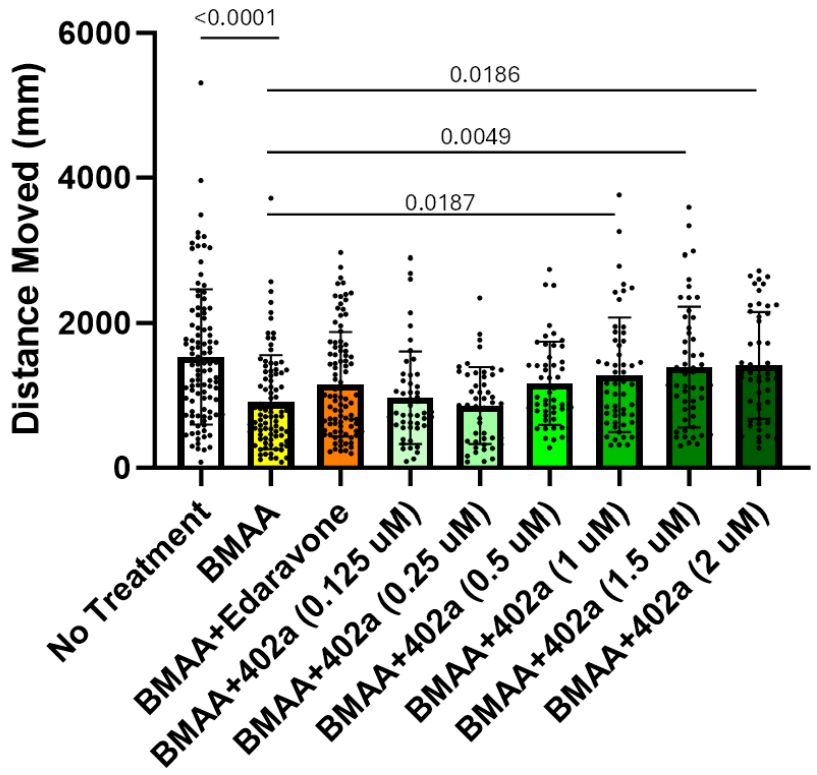

Figure 3. Dose response of Cannflavin A (402a) in a BMAA-induced model of neurotoxicity in zebrafish larvae. Experiments were done with seven biological replicates.

Data Quality

Quality control assessment through boxplot visualization (Supplementary Material: Plots) confirmed excellent data consistency across the biological replicates within each condition group. The normalized gene expression counts displayed remarkably uniform distribution patterns, with median expression levels precisely aligned across all six replicates for each condition, indicating successful normalization and comparable library sizes. The characteristic compression of interquartile ranges near zero reflects the expected transcriptomic landscape where the majority of genes exhibit low to moderate expression levels. Consistent outlier patterns extending to approximately 500,000 normalized counts were observed across all

samples, representing highly expressed genes such as housekeeping proteins that were reproducibly detected. This uniform distribution profile, combined with the absence of sample-specific technical artifacts or batch effects, demonstrates robust experimental reproducibility and validates the dataset's suitability for downstream differential expression analysis. The boxplot patterns align with established quality standards for normalized RNA-seq data, confirming that technical variation has been effectively minimized while preserving genuine biological signals.

The sample correlation analysis (Figure 4**)** demonstrated high reproducibility within experimental groups, with control samples showing strong internal correlations ($r > 0.90$). Treatment groups exhibited distinct expression profiles compared to controls, as evidenced by the hierarchical clustering pattern that segregated samples by treatment condition. The overall correlation structure supports the validity of the experimental design and suggests that the observed gene expression changes are treatment-specific rather than due to technical variability.

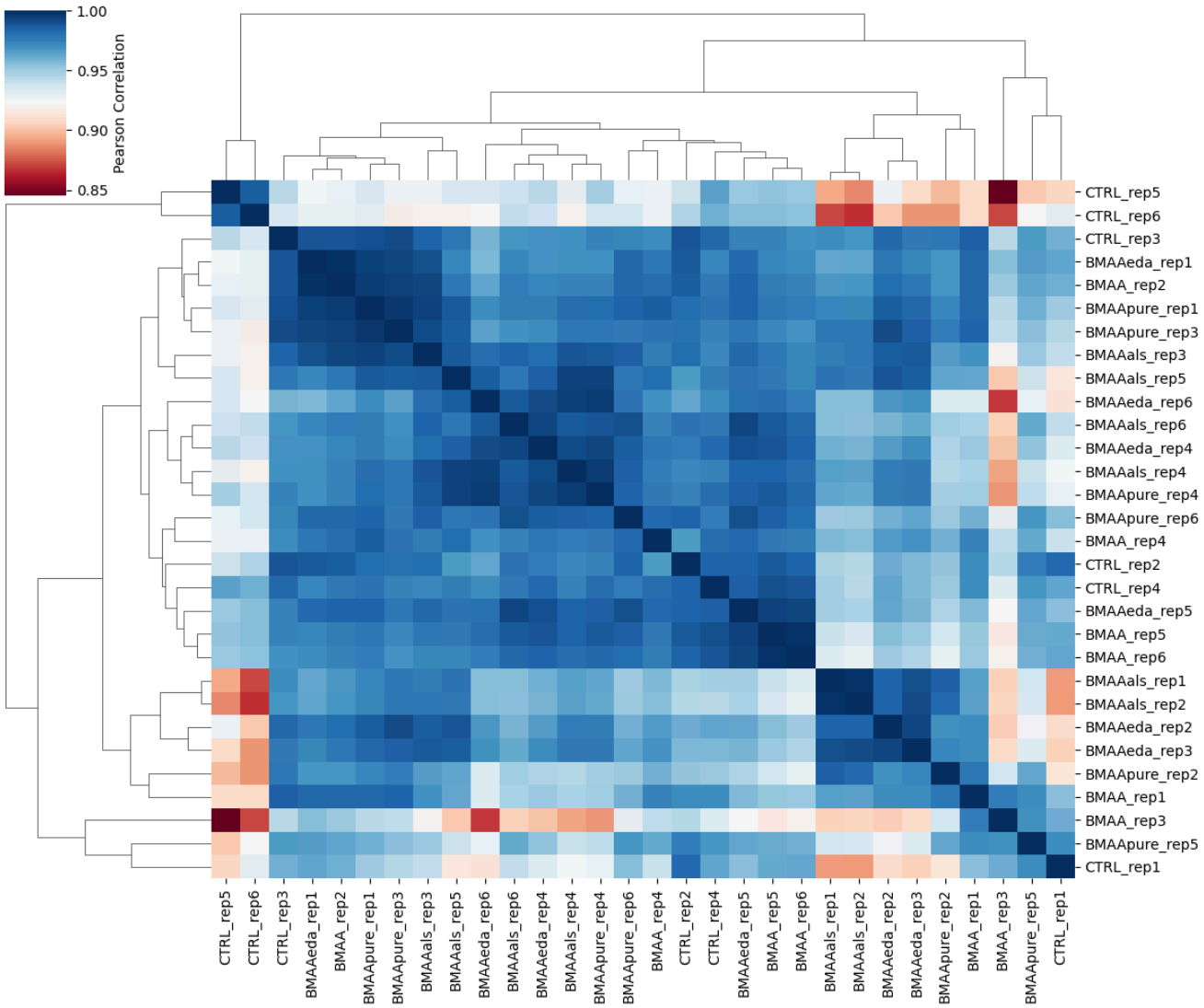

Figure 4. Heatmap showing pairwise Pearson correlations of gene expression between all samples, clustered hierarchically. A darker blue square indicates a stronger positive correlation, as seen in the squares along the diagonal showing a perfect self-correlation (r =1.0).

The principal component analysis (Supplementary Material: Plots) revealed substantial variability in gene expression profiles across experimental conditions. Notably, control samples showed considerable dispersion across the PCA space, with replicates distributed from the bottom region (PC1 >= 150, PC2 ≈−150) to the upper right quadrant (PC1 ≈150, PC2 ≈50),

indicating significant baseline heterogeneity in untreated samples. BMAA treatment and therapeutic interventions (CNR401, Edaravone, and Cannflavin A) showed similarly dispersed patterns across both principal components, which together explain 38.04% of the total variance. This observed variability in RNA-seq data aligns with established norms [23].

Differentially Expressed Genes

Differential gene expression analysis between BMAA-affected and treated conditions revealed distinct therapeutic responses across the three neuroprotective compounds (Figures 5-6). CNR-401 treatment resulted in 1,576 significantly differentially expressed genes, while Edaravone treatment showed 359 differentially expressed genes, and Cannflavin A treatment demonstrated 130 differentially expressed genes (Table 1). These findings indicate varying degrees of transcriptomic modulation, with CNR-401 exhibiting the most extensive gene expression changes relative to BMAA-affected conditions.

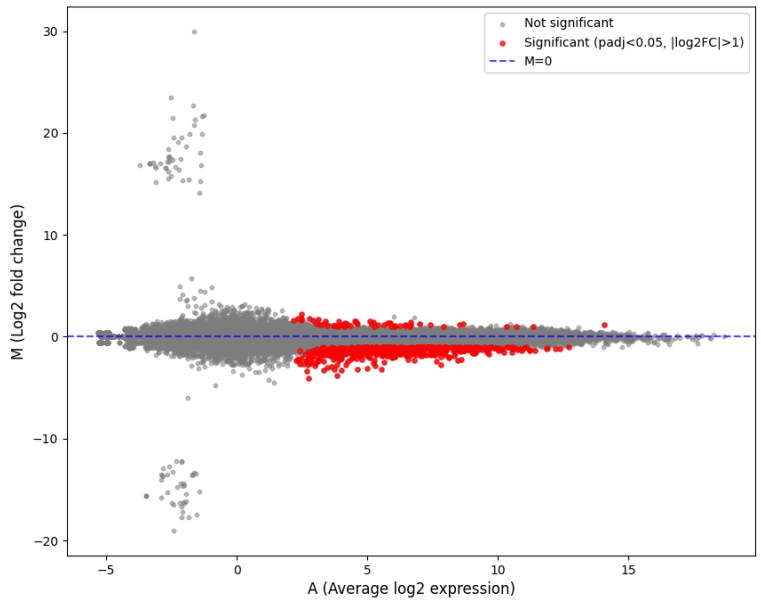

(a) BMAA-Affected vs Control

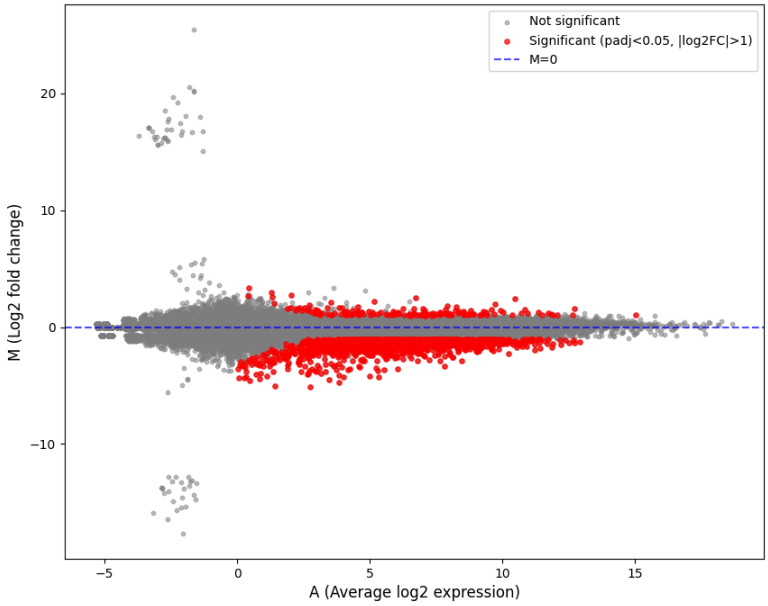

(b) BMAA-Affected vs CNR-401-Treated

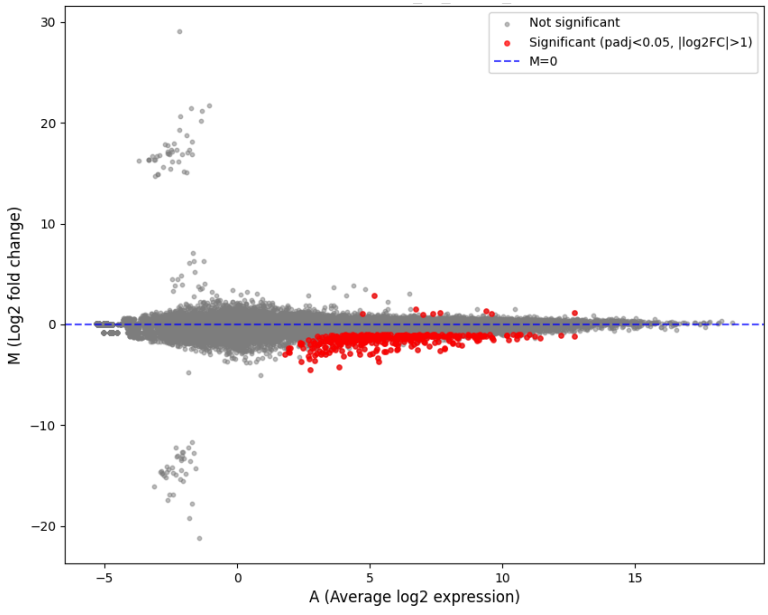

(c) BMAA-Affected vs Edaravone-Treated

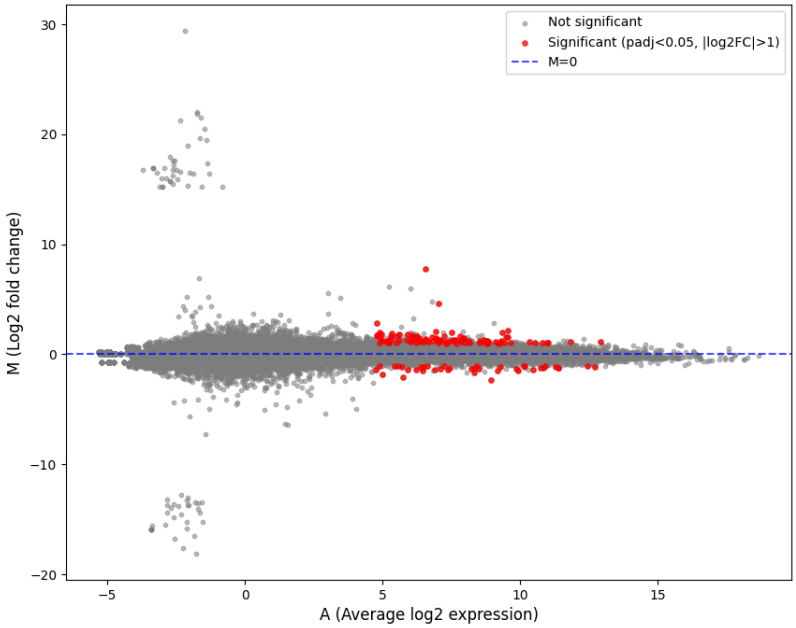

(d) BMAA-Affected vs Cannflavin A-Treated

Figure 5. MA plots showing differential gene expression analysis between BMAA-affected and treated conditions. Each point represents a gene plotted by average log expression (A, x-axis) versus log2 fold change (M, y-axis). Red points indicate significant differentially expressed genes.

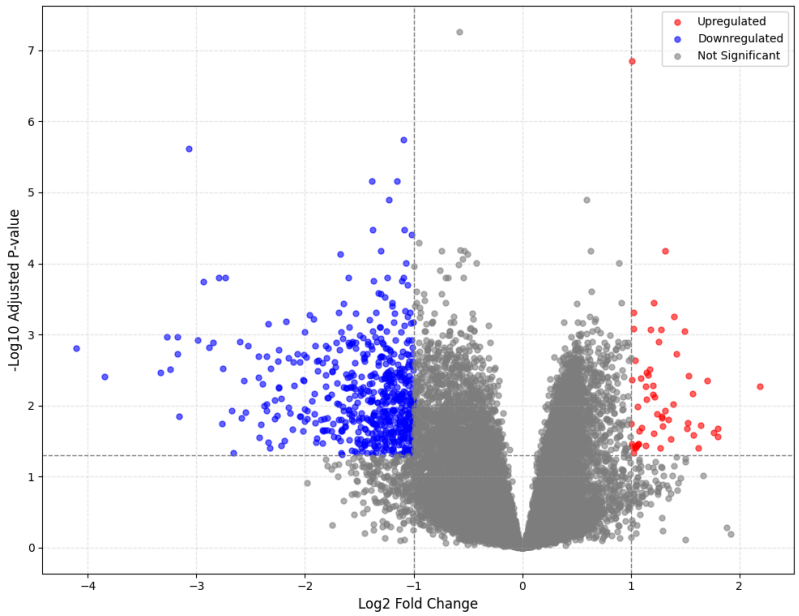

(a) BMAA-Affected vs Control

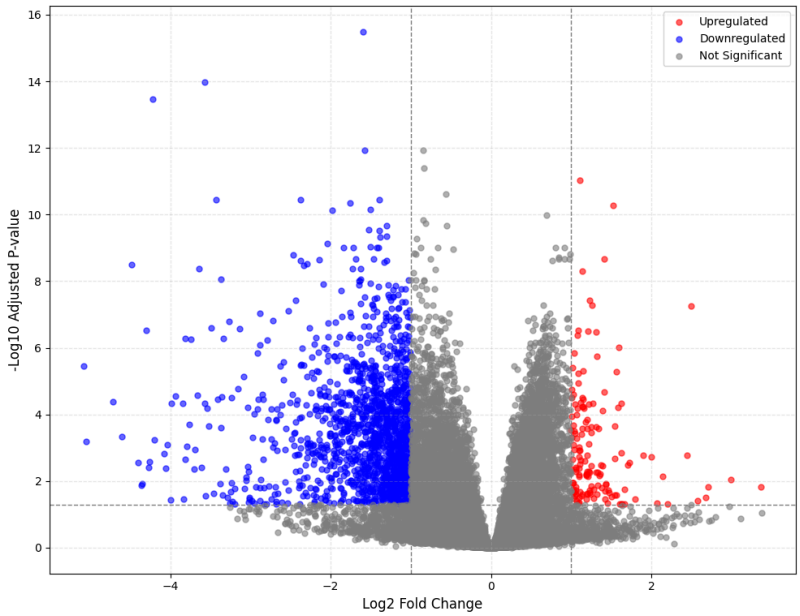

(b) BMAA-Affected vs CNR-401-Treated

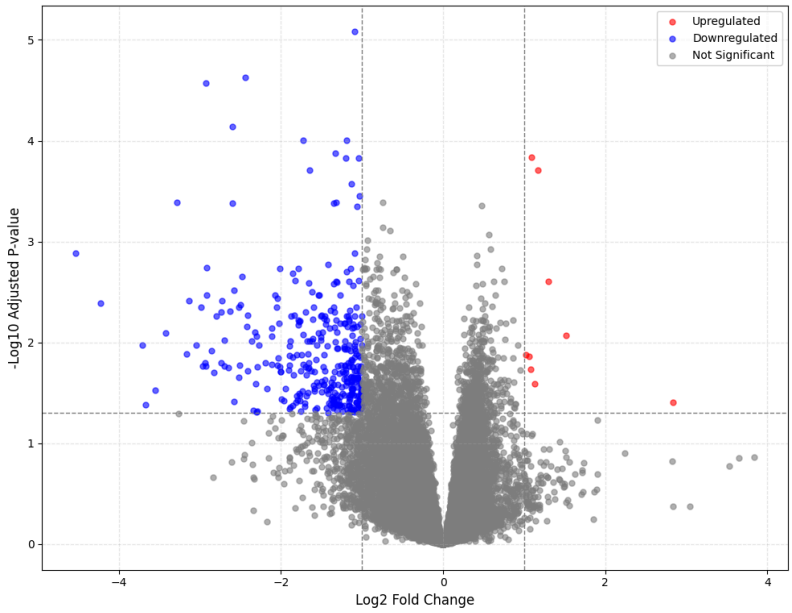

(c) BMAA-Affected vs Edaravone-Treated

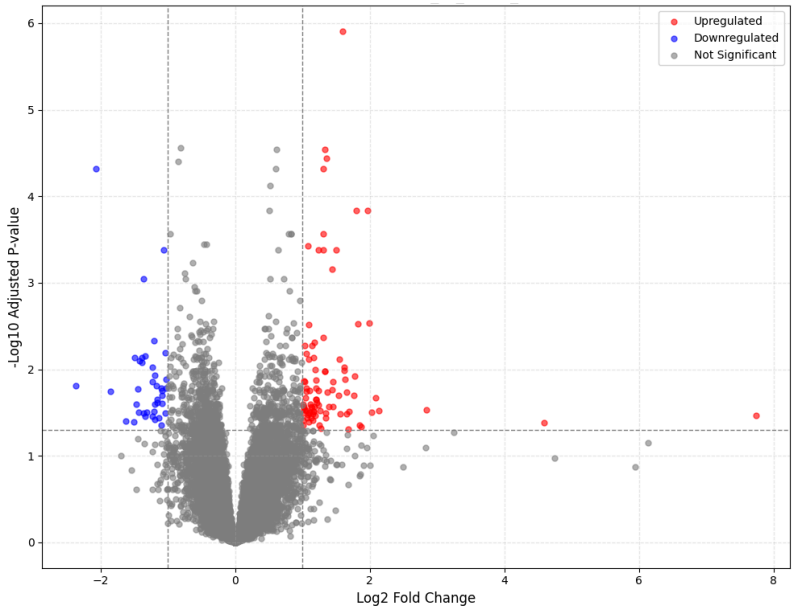

(d) BMAA-Affected vs Cannflavin A-Treated

Figure 6. Volcano plots displaying statistical significance versus biological significance of differential gene expression. Each point represents a gene plotted by log2 fold change (x-axis)

versus -log10 adjusted p-value (y-axis). Blue points indicate significantly downregulated genes, red points indicate significantly upregulated genes.

Table 1. Summary of pairwise comparisons of interest.

Comparison	Total Genes	Significant Genes	Upregulated	Downregulated
BMAA vs Control	28788	624	57	567
BMAA vs BMAA + CNR401	28788	1576	149	1427
BMAA vs BMAA + Edaravone	28788	359	9	350
BMAA vs BMAA + Cannflavin A	28788	130	91	39

Ortholog Mapping

Mapping the significantly expressed DEGs from the BMAA-affected vs CNR-401-treated comparison revealed that the top 19 genes belonged to the *UGT* Gene Family and were all downregulated (Table 2). It is important to note that these 19 human UGT genes mapped from the same underlying zebrafish gene transcripts, explaining the identical or nearly identical expression values. This ortholog mapping thus indicates a coordinated downregulation of the *UGT* family rather than independent measurements. In the BMAA vs control comparison, this family of orthologs showed only approximately a -0.5 log2foldchange (Supplementary Material: Data), demonstrating the significant impact of CNR-401 on these pathways.

Table 2. The top 30 human orthologs (sorted by L2FC) differentially expressed when BMAA-affected samples were treated with CNR401.

Ortholog Name	Description	Absolute L2FC	Expression	Adjusted P-Value
UGT2B10	UDP glucuronosyltransferase family 2 member B10	4.077694	Downregulated	0.001473
UGT2A3	UDP glucuronosyltransferase family 2 member A3	4.077694	Downregulated	0.001473
UGT2B28	UDP glucuronosyltransferase family 2 member B28	4.077694	Downregulated	0.001473
UGT3A1	UDP glycosyltransferase family 3 member A1	4.077694	Downregulated	0.001473
UGT2B4	UDP glucuronosyltransferase family 2 member B4	4.077694	Downregulated	0.001473
UGT1A6	UDP glucuronosyltransferase family 1 member A6	4.077694	Downregulated	0.001473

UGT2B7	UDP glucuronosyltransferase family 2 member B7	4.077694	Downregulated	0.001473
UGT2A1	UDP glucuronosyltransferase family 2 member A1 complex locus	4.077694	Downregulated	0.001473
UGT2B15	UDP glucuronosyltransferase family 2 member B15	4.077694	Downregulated	0.001473
UGT2B17	UDP glucuronosyltransferase family 2 member B17	4.077694	Downregulated	0.001473
UGT2B11	UDP glucuronosyltransferase family 2 member B11	4.077694	Downregulated	0.001473
UGT1A9	UDP glucuronosyltransferase family 1 member A9	4.077694	Downregulated	0.001473
UGT1A8	UDP glucuronosyltransferase family 1 member A8	4.077694	Downregulated	0.001473

UGT1A10	UDP glucuronosyltransferase family 1 member A10	4.077694	Downregulated	0.001473
UGT1A7	UDP glucuronosyltransferase family 1 member A7	4.077694	Downregulated	0.001473
UGT1A4	UDP glucuronosyltransferase family 1 member A4	4.077694	Downregulated	0.001473
UGT2A2	UDP glucuronosyltransferase family 2 member A2	4.077694	Downregulated	0.001473
UGT1A3	UDP glucuronosyltransferase family 1 member A3	4.077694	Downregulated	0.001473
UGT1A5	UDP glucuronosyltransferase family 1 member A5	4.077694	Downregulated	0.001473
URGCP	upregulator of cell proliferation	3.702947	Downregulated	0.004319
DAO	D-amino acid oxidase	3.68739	Downregulated	0.001132

SDR42E2	short chain dehydrogenase/reductase family 42E; member 2	3.663107	Downregulated	2.679562886399305e-05
GBP6	guanylate binding protein family member 6	3.558249	Downregulated	0.028347
MXRA5	matrix remodeling associated 5	3.424166	Downregulated	3.619114816823018e-11
NOTCH4	notch receptor 4	3.15797	Downregulated	1.658254919506955e-05
B3GALT9	beta-1;3-galactosyltransferase 9	3.018835	Downregulated	0.005205
HLA-DQA1	major histocompatibility complex; class II; DQ alpha 1	3.016801	Downregulated	0.034057
HLA-DQA2	major histocompatibility complex; class II; DQ alpha 2	3.016801	Downregulated	0.034057
UNG	uracil DNA glycosylase	2.996153	Upregulated	0.009045

COL6A3	collagen type VI alpha 3 chain	2.950076	Downregulated	9.900582448395986e-05

Functional Enrichments

Gene ontology (GO) biological process enrichment analysis revealed that, in the BMAA versus BMAA+CNR401 comparison (Figure 7b), the most significantly enriched terms included extracellular matrix organization, external encapsulating structure organization, cellular response to cytokine stimulus, extracellular structure organization, cytokine-mediated signaling pathway, steroid metabolic process, estrogen metabolic process, calcium-mediated signaling, inflammatory response, and regulation of angiogenesis. For the BMAA versus control comparison (Figure 7a), enriched GO biological processes included cellular response to cytokine stimulus, cellular response to growth hormone stimulus, growth hormone receptor signaling pathway, cytokine-mediated signaling pathway, extracellular matrix organization, sulfation, ethanol catabolic process, positive regulation of receptor signaling pathway via STAT, ethanol metabolic process, and external encapsulating structure organization.

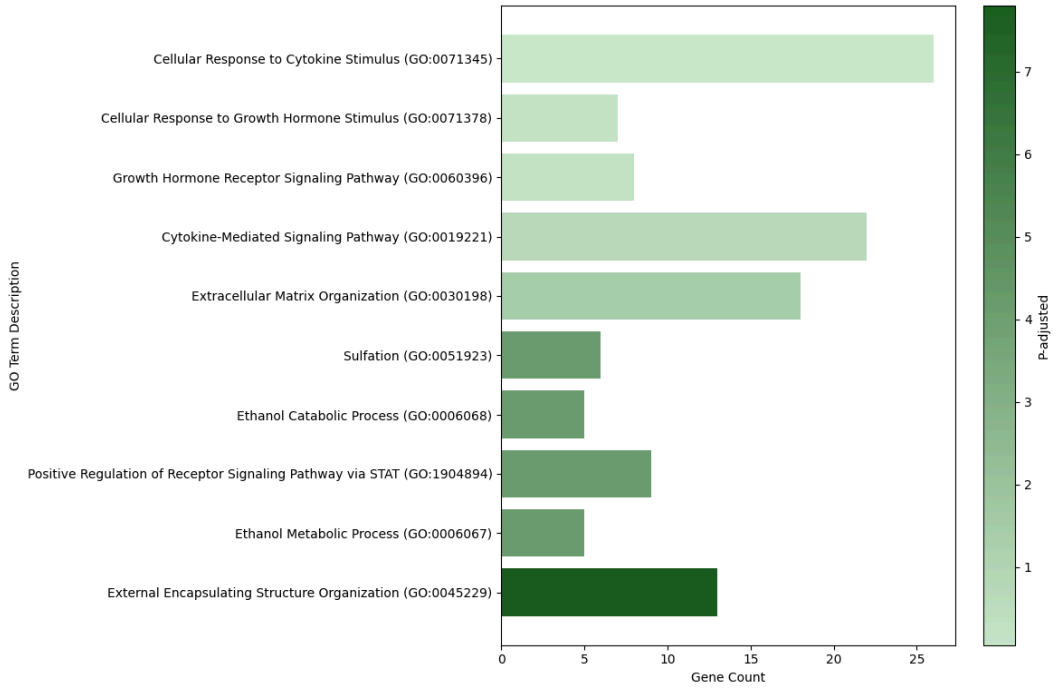

297

298 (a) BMAA-Affected vs Control

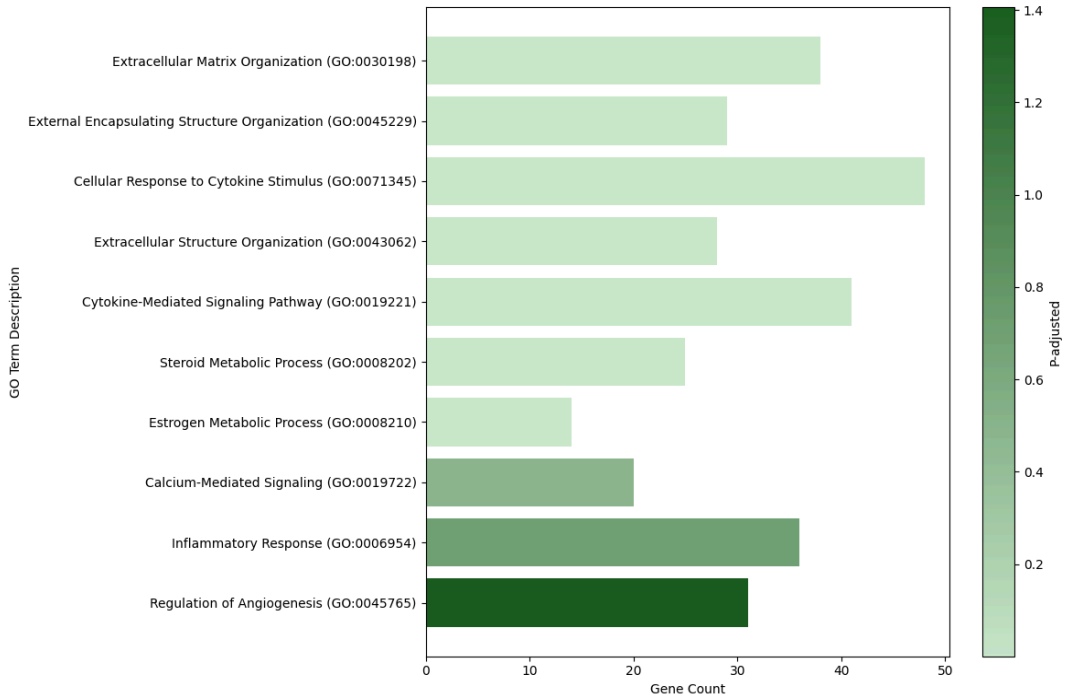

299

300 **(b)** BMAA-Affected vs CNR-401 Treated

Figure 7. GO biological process (BP) enrichment analysis of differentially expressed genes between pairwise comparisons of interest. Bar length indicates the number of genes associated with each enriched GO term, while color intensity reflects the adjusted p-value for enrichment significance.

Kyoto Encyclopedia of Genes and Genomes (KEGG) enrichment analysis showed that, in the BMAA versus BMAA+CNR401 comparison **(**Figure 8b**)**, the top enriched pathways were cytokine-cytokine receptor interaction, steroid hormone biosynthesis, ascorbate and aldarate metabolism, porphyrin and chlorophyll metabolism, pentose and glucuronate interconversions, bile secretion, PI3K-Akt signaling pathway, metabolism of xenobiotics by cytochrome P450, ovarian steroidogenesis, and retinol metabolism. In the BMAA versus control comparison (Figure 8a), enriched KEGG pathways included JAK-STAT signaling pathway, PI3K-Akt signaling pathway, pathways in cancer, cytokine-cytokine receptor interaction, ovarian steroidogenesis, ECM-receptor interaction, Th17 cell differentiation, choline metabolism in cancer, human papillomavirus infection, and small cell lung cancer.

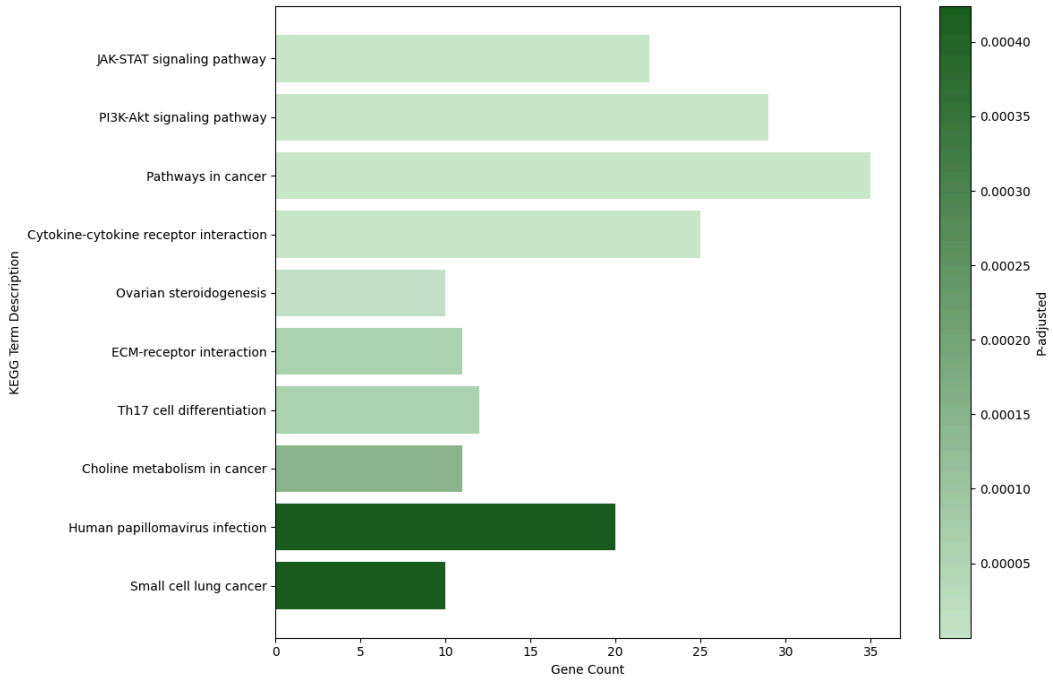

315

316 **(a)** BMAA-Affected vs Control

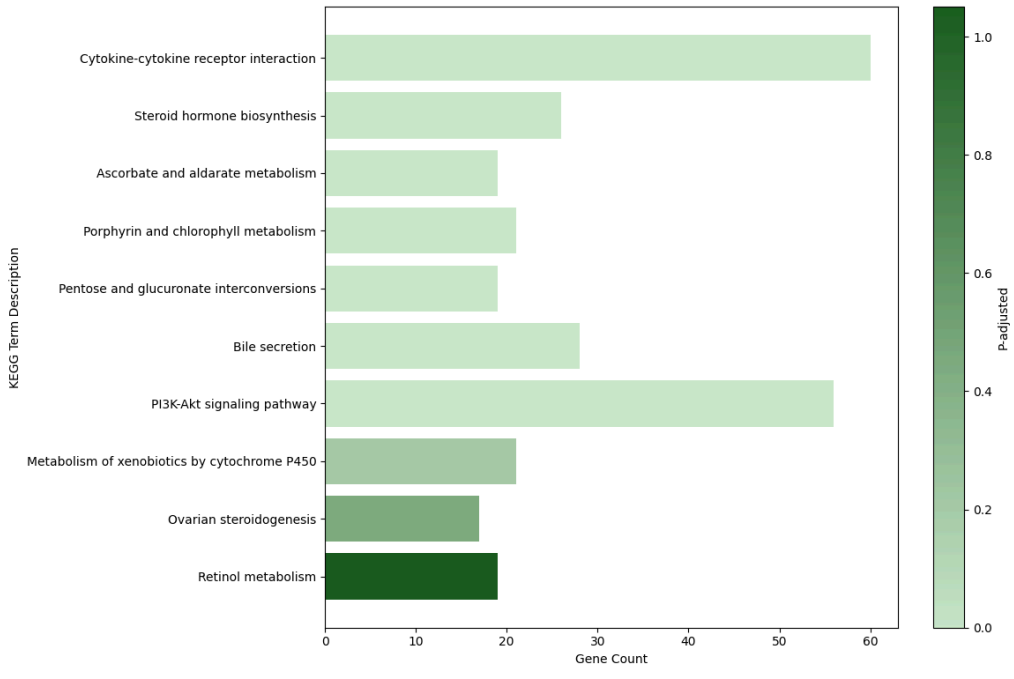

317

318 **(b)** BMAA-Affected vs CNR-401-Treated

Figure 8. KEGG pathway enrichment analysis of differentially expressed genes in each experimental comparison. Bar length represents the number of genes associated with each enriched pathway, and color intensity reflects the adjusted p-value for statistical significance.

DISCUSSION

CNR-401 Induces Broad Transcriptomic Changes in BMAA-Exposed Zebrafish

Our analysis revealed that CNR-401 treatment produces a strikingly extensive alteration in gene expression profiles compared to BMAA-alone exposure or subsequent treatment with other therapies. In the BMAA vs. BMAA + CNR-401 comparison, 1,576 genes were significantly differentially expressed, far exceeding the 359 DEGs observed with Edaravone and 130 with Cannflavin A. This indicates that CNR-401 elicits a broad transcriptomic response in the ALS model. Notably, the vast majority of CNR-401–modulated genes (1427 genes) were downregulated relative to BMAA-alone, with only 149 upregulated. This pattern suggests that CNR-401 largely counteracts or normalizes many of the gene expression changes induced by BMAA. In other words, genes pathologically elevated in the BMAA condition tend to be suppressed by CNR-401, pointing to a robust mitigation of BMAA-driven molecular perturbations. Such a widespread reversal of BMAA effects implies that CNR-401 engages multiple biological pathways, consistent with a multi-target mechanism of neuroprotection. In contrast, Edaravone and Cannflavin A triggered comparatively modest transcriptomic shifts, highlighting that CNR-401's impact is both broader and more potent in this model. The fact that CNR-401 rescued diseased zebrafish in the functional mobility analysis at least confirms that this breadth of gene regulation is not harmful and instead may translate into a more comprehensive

therapeutic effect, as ALS pathology involves myriad dysregulated processes. However, this large amount of genetic changes does warrant careful interpretation.

Top Differentially Expressed Genes Reveal CNR-401's Multi-Target Neuroprotective Mechanisms

Several of the most dysregulated genes in the CNR-401 treatment group have clear links to ALS pathophysiology. *UDP-glucuronosyltransferase (UGT)* family members dominated the top-ranked DEGs. UGTs are Phase II detoxification enzymes responsible for glucuronidation of endogenous toxins and xenobiotics [25]. One explanation of their coordinated suppression suggests that CNR-401 reduced the need for BMAA detoxification via glucuronidation. In this interpretation, CNR-401 aids in neutralizing or clearing BMAA (or its toxic metabolites) by other means, thereby reducing reliance on endogenous UGT-mediated glucuronidation. In essence, if BMAA exposure alone induces *UGT* expression as a compensatory detox response, the addition of CNR-401 appears to alleviate that stress, resulting in lower UGT levels. A second interpretation supported by the functional enrichments is that the suppression of *UGT* genes reduces their known conjugation and elimination of steroids, thereby increasing levels of endogenous neuroprotective steroids, discussed later.

Several other ALS-relevant genes were significantly downregulated by CNR-401, aligning with beneficial modulation of neuroinflammatory and neurodegenerative pathways. *URGCP* (Upregulator of Cell Proliferation) was one such gene. URGCP is a cell-cycle regulator that drives proliferation via Wnt/β-catenin signaling [25], and its reduction in the CNR-401 group is particularly noteworthy. In ALS, excessive proliferation of glial cells (astrocytes and microglia)

contributes to neuroinflammation and scarring [26]; therefore *URGCP* downregulation may help curb this pathological gliosis. Indeed, suppression of URGCP/Wnt signaling has been shown to dampen microglial activation and neuroinflammation in the spinal cord [27], suggesting that CNR-401 creates a more quiescent glial environment.

Another key gene, *DAO (D-amino acid oxidase)*, was also markedly downregulated, consistent with neuroprotective mechanisms observed in ALS models. It has been demonstrated that *DAO* inactivation in astrocytes reduces D-serine-mediated excitotoxicity, protecting motor neurons [28]. However, DAO loss-of-function mutations in neurons have been linked to elevated D-serine and neurodegeneration [29], highlighting context-dependent effects. CNR-401-induced DAO suppression may reflect astrocyte-specific modulation, a complex feedback mechanism, or a time-dependent effect – for example, if BMAA exposure had suppressed D-serine availability, lowering DAO could be a compensatory attempt to restore normal neurotransmission. Additionally, CNR-401's other actions (e.g. anti-glutamatergic or antioxidant effects) might buffer the impact of increased D-serine in neurons. These findings underscore the intricacy of excitotoxic pathways in ALS and suggest that while CNR-401 broadly mitigates BMAA toxicity, certain aspects like D-serine metabolism require further investigation. Despite this complexity, the functional mobility data showed that CNR-401 treatment rescues BMAA-induced motor deficits, suggesting that any potential risks associated with altered D-serine metabolism are indeed outweighed by the compound's overall neuroprotective effects in vivo.

MXRA5 (Matrix Remodeling Associated 5) was already slightly downregulated in BMAA-exposed zebrafish compared to control (Supplementary Material: Data), but treatment

with CNR-401 caused a much greater suppression. *MXRA5* is involved in extracellular matrix (ECM) remodeling and can facilitate MMP-9 activation, contributing to breakdown of the blood-spinal cord barrier and tissue damage [30]. The pronounced suppression of this gene therefore suggests that CNR-401 enhances a protective response. This suppression likely reflects modulation of the well-established TGF-β1 pathway, which controls *MXRA5* expression and ECM homeostasis [31]. Our GO enrichment analysis strongly supports this hypothesis by identifying extracellular matrix organization processes among the most significantly enriched terms in the CNR-401 group, indicating that therapeutic effects are largely mediated by the restoration of ECM stability. Reduced *MXRA5* expression is part of this larger protective modulation of the ECM, leading to reduced extracellular proteolysis and a more intact neurovascular unit, thereby protecting motor neurons from inflammatory infiltration and toxic exposure.

Both *HLA-DQA1* and *HLA-DQA2*, major *histocompatibility complex (MHC) class II immune genes*, were also among the top downregulated transcripts. Both proteins modulate immune responses with the HLA-DQA1 protein forming a functional complex with HLA-DQB1 to create an antigen-binding heterodimer that displays foreign peptides derived from extracellular proteins to the immune system [32], and HLA-DQA2 modulating immune responses through non-classical pathways [33]. In the central nervous system, MHC class II molecules like HLA-DQ are typically absent under healthy conditions but become upregulated on microglia during neuroinflammatory processes, making them key markers of activated immune cells in the brain [34]. Lower *HLA-DQ* expression therefore suggests suppression of neuroimmune activation in treated zebrafish. This aligns with CNR-401's general anti-inflammatory signature,

as reduced *MHC II* expression limits the activation of CD4+ T cells and the transition of microglia from a resting to a reactive, pro-inflammatory state in the CNS. Along with *URGCP* and *MXRA5*, the downregulation of *HLA-DQA1* and *HLA-DQA2* reinforces the notion that CNR-401 dampens processes that contribute to neuroinflammation and the neurodegenerative environment.

In contrast to the many downregulated genes, *UNG (Uracil-DNA glycosylase)* stood out as one of the few upregulated genes. *UNG* is a DNA repair enzyme involved base-excision repair that removes uracil from DNA, thereby correcting cytosine deamination and other oxidative DNA damage [35]. Its upregulation by CNR-401 suggests an enhanced capacity for genomic maintenance in response to BMAA toxicity and associated oxidative stress, which inflicts DNA damage in neurons [36]. Given that accumulated DNA damage in motor neurons is a known contributor to ALS progression [37], this pro-repair response would be neuroprotective.

Collectively, the top DEGs indicate that CNR-401 treatment modulates key players in detoxification and steroid metabolism (*UGT* genes), cell proliferation/inflammation (*URGCP, HLA-DQA1, HLA-DQA2*), excitotoxic signaling (*DAO*), matrix integrity (*MXRA5*), and genomic stability (*UNG*). Such changes are broadly consistent with a therapeutic shift toward neuroprotection – reducing toxic exposures, calming injurious immune activity, preserving structural support, and bolstering repair mechanisms.

Enriched Biological Processes: ECM Organization and Inflammation

The differential expression patterns translate into clear enrichment of biological processes and pathways relevant to ALS. The Gene Ontology enrichment analysis reveals a compelling

convergence of two fundamental pathological processes that serve as immediate contributors to motor neuron degeneration in ALS: inflammatory response and extracellular matrix (ECM) organization. These processes represent the most direct mechanisms by which BMAA initiates motor neuron injury and how CNR-401 subsequently counteracts these damaging processes.

The enrichment of ECM organization terms “extracellular matrix organization”, “external encapsulating structure organization”, and “extracellular structure organization” in our analysis directly reflects the mechanistic foundation of ALS pathology described in the literature. Research of the related neurodegenerative disease multiple sclerosis (MS) has demonstrated that many ECM components elevated during tissue damage are inherently pro-inflammatory and enhance inflammatory processes [38]. Within the context of ALS, breakdown of the extracellular matrix represents a critical initiating event that triggers a cascade of inflammatory responses leading to motor neuron degeneration [39]. In healthy neural tissue, stable ECM and basement membranes provide structural support that maintains microglia in a ramified, quiescent state. However, when ECM breakdown occurs, microglia become mobile and reactive, further degrading the already compromised extracellular matrix and establishing a chronic para-inflammatory state in the motor tracts [39]. This creates a self-perpetuating cycle where ECM damage promotes inflammation, which in turn exacerbates ECM degradation.

This prominent enrichment of inflammatory response processes was captured in our Gene Ontology analysis, which showed "inflammatory response", "cytokine-mediated signaling pathway", and "cellular response to cytokine stimulus" among the most significant terms. This provides compelling evidence for neuroinflammation’s central role in ALS pathogenesis. The

convergence of inflammatory processes aligns with extensive research that demonstrates neuroinflammation as a fundamental mechanism that drives motor neuron injury rather than merely a secondary consequence of neurodegeneration. Motor neuron degeneration in ALS operates through non-cell autonomous mechanisms, where motor neuron death results not solely from intrinsic cellular defects but from active contributions of surrounding glial cells. This concept has been definitively established through chimeric mouse studies demonstrating that wild-type neurons acquire ALS phenotypes when surrounded by glial cells expressing mutant proteins, confirming that the cellular environment directly determines motor neuron survival [40]. Neuroinflammation in ALS is characterized by coordinated activation of multiple immune and glial populations that directly contribute to motor neuron degeneration. This inflammatory milieu includes infiltration of peripheral lymphocytes and macrophages, widespread activation of resident microglia and reactive astrocytes, and engagement of complement cascades that collectively contribute to motor neuron death through the coordinated release of pro-inflammatory cytokines, reactive oxygen species, and other neurotoxic factors [41]. The neuroinflammatory response transforms the normally supportive glial environment into one that actively promotes motor neuron degeneration, establishing neuroinflammation as a primary therapeutic target for disease-modifying interventions in ALS [41].

The observation that inflammatory response and ECM organization are enriched processes in both BMAA toxicity and CNR-401 treatment provides compelling evidence for a coherent pathological and therapeutic narrative. This shared enrichment demonstrates that these biological processes constitute the core molecular battleground where neurodegeneration occurs and where therapeutic intervention must be focused. The initial exposure to BMAA triggers ECM

degradation and neuroinflammation that directly damages motor neurons. Then, subsequent CNR-401 treatment appears to target these same fundamental pathways, suggesting that this therapeutic specifically addresses the root mechanisms of BMAA-induced motor neuron injury. While BMAA disrupts these systems through toxic mechanisms, CNR-401's multi-target botanical approach modulates the same pathways through protective mechanisms. The therapeutic enrichment of these pathways likely represents CNR-401's dual capacity to stabilize ECM integrity while simultaneously modulating inflammatory responses to create a more permissive environment for motor neuron survival and potential regeneration. This convergence of pathological initiation and therapeutic intervention on identical biological processes underscores the mechanistic precision of CNR-401's therapeutic approach and validates the fundamental importance of ECM organization and inflammatory response as direct contributors to motor neuron injury in ALS.

Enriched Biological Processes: Calcium Signaling and Steroid Metabolism

The Gene Ontology enrichment of calcium-mediated signaling and steroid metabolic processes represents a secondary tier of regulatory mechanisms that modulate cellular stress responses and provide neuroprotective functions in ALS pathogenesis. These pathways operate as crucial modulators of cellular homeostasis, influencing both the susceptibility to neurodegeneration and the capacity for neuroprotective responses following initial ECM and inflammatory damage.

Motor neurons in ALS exhibit fundamental vulnerabilities in calcium homeostasis that predispose them to calcium-mediated toxicity. These neurons express high levels of calcium-permeable AMPA receptors while maintaining low calcium buffering capacity, creating

susceptibility to intracellular calcium overload [42]. This calcium dysregulation operates through a "toxic shift" [43] within the endoplasmic reticulum-mitochondria calcium cycle, representing a key mechanism in motor neuron degeneration. The chronic excitotoxicity mediated by AMPA receptors initiates a self-perpetuating process of intracellular calcium dysregulation with consecutive endoplasmic reticulum calcium depletion and mitochondrial calcium overload, ultimately spiraling toward catastrophic levels of cytosolic calcium [43, 44]. The enrichment of "calcium-mediated signaling" in the CNR-401 versus BMAA comparison provides molecular evidence for CNR-401's potential therapeutic effects through modulation of these fundamental cellular stress response mechanisms that are compromised in ALS pathology.

The emergence of steroid metabolic process and specifically estrogen metabolic process in GO enrichment correlates with the downregulation of *UGT (UDP-glucuronosyltransferase)* enzymes that conjugate steroid hormones, and reflects CNR-401's anti-catabolic influence on critical endogenous neuroprotective mechanisms. The central nervous system possesses capacity for local steroid synthesis, producing progesterone, testosterone, and estradiol that provide neuroprotective effects independent of peripheral hormonal sources [45, 46]. For example, one such neurosteroid is allopregnanolone, a progesterone metabolite that demonstrates neuroprotective properties through mechanisms including GABA-A receptor modulation, anti-apoptotic signaling, and neuroinflammation regulation [46, 47]. Estrogen metabolism pathways are particularly relevant to ALS, demonstrating anti-apoptotic mechanisms, calcium homeostasis regulation, microglial modulation, anti-inflammation, and antioxidant activities [48, 49]. Specific examples include 17β-estradiol which demonstrates direct protective effects on spinal motor neurons through anti-apoptotic and anti-inflammatory actions on glial cells [50],

and estrogen signaling mediated by G-protein-coupled receptor 30 (GPR30) which demonstrates similar anti-apoptotic effects on motor neurons [51]. The downregulation of steroid-conjugating enzymes by CNR-401 suggests a sophisticated therapeutic strategy that enhances the bioavailability and duration of action of endogenous neuroprotective steroids. This mechanism provides a molecular explanation for how botanical therapeutics can enhance natural neuroprotective responses without requiring exogenous hormone supplementation.

The enrichment of both calcium and steroid processes suggests that CNR-401 targets these interconnected regulatory systems to provide comprehensive neuroprotective effects. By modulating calcium homeostasis while potentially enhancing neurosteroid bioavailability, CNR-401 appears to restore cellular capacity for adaptive responses to pathological stimuli while enhancing endogenous neuroprotective mechanisms that are compromised in ALS progression. These enriched terms represent sophisticated therapeutic targets that address multiple levels of cellular dysfunction, explaining how botanical therapeutics can simultaneously target excitotoxicity, neuroinflammation, and cellular stress responses.

KEGG Pathway Enrichment Reinforces GO Biological Process and Gene Expression Findings

KEGG pathway enrichment analysis reinforces these GO biological process findings. After CNR-401 treatment, “cytokine–cytokine receptor interaction” was the top pathway, directly supporting the GO enrichment of inflammatory response processes and confirming that CNR-401’s therapeutic mechanism involves comprehensive modulation of immune signaling networks that drive neuroinflammation in ALS pathogenesis. This pathway enrichment indicates

that CNR-401 affects not only individual cytokine expression but the broader intercellular communication systems that perpetuate chronic neuroinflammatory states.

Furthermore, the enrichment of the "steroid hormone biosynthesis" and "ovarian steroidogenesis" pathways directly reinforces the previous interpretation that CNR-401 enhances the bioavailability and persistence of endogenous neuroprotective steroids. These KEGG pathways capture the broader metabolic context in which UGT downregulation operates, highlighting that the transcriptomic impact of CNR-401 extends beyond isolated gene effects to coordinated modulation of entire steroidogenic networks. This systemic enrichment supports the conclusion that CNR-401 not only reduces steroid catabolism via *UGT* suppression but also potentially upregulates or stabilizes upstream biosynthetic processes, thereby amplifying the pool of neuroactive steroids available to exert anti-inflammatory, anti-apoptotic, and neuroprotective functions relevant to ALS pathophysiology.

Appearance of "ascorbate and aldarate metabolism" and "retinol metabolism" among enriched pathways provides mechanistic insight into CNR-401's antioxidant capabilities, complementing the GO enrichment of calcium signaling and steroid metabolic processes, and the marked downregulation of *DAO*. Ascorbate (vitamin C) is a major direct antioxidant and free radical scavenger in the central nervous system [52, 53], playing a critical role in neutralizing reactive oxygen species and protecting neurons from the oxidative stress in ALS pathogenesis. Similarly, retinol metabolism enrichment indicates modulation of vitamin A, an indirect antioxidant [54]. Both vitamins A and C have been highlighted as natural antioxidants with the potential to suppress neural oxidative damage and slow neurodegeneration in ALS [55].

Two metabolic pathways—"pentose and glucuronate interconversions" and "metabolism of xenobiotics by cytochrome P450"—directly relate to the detoxification effect and the coordinated downregulation of UGT enzymes discussed previously. The pentose and glucuronate interconversions pathway represents a fundamental phase II detoxification mechanism [56] and the central biochemical process within this pathway, glucuronidation, is primarily catalyzed by UDP-glucuronosyltransferase (UGT) enzymes [57]. This evidence thus demonstrates that CNR-401 fundamentally alters cellular detoxification capacity by targeting both the enzymatic machinery (UGT downregulation) and the broader metabolic framework (pathway enrichment) of Phase II conjugation processes. Transcriptomic analyses across multiple species have consistently identified metabolism of xenobiotics by cytochrome P450 as a major Phase I pathway intersecting with the broader detoxification processes [58, 59]. The enrichments of these two pathways thus provide systems-level evidence that CNR-401 reduces the metabolic burden of toxin processing, with cytochrome P450 enzymes catalyzing Phase I oxidative metabolism and glucuronidation serving as a critical Phase II conjugation step that enhances the water solubility and excretion of metabolites [59].

Novel Pathway Identified by KEGG and Comparison to Control

Beyond validating GO enrichment findings, KEGG analysis revealed additional therapeutic mechanisms not captured in biological process enrichment. The enrichment of the PI3K-Akt signaling pathway represents a critical finding, as this pathway serves as a central regulator of neuronal survival and has been extensively implicated in neuroprotective mechanisms across numerous neurodegenerative diseases [60]. The PI3K-Akt pathway plays a pivotal role in

neuroprotection by promoting cell survival through stimulation of cell proliferation and inhibition of apoptosis, and modulation of cellular stress responses including oxidative stress and inflammatory signaling [61]. In ALS pathogenesis specifically, studies using SOD1-G93A ALS mouse models have shown that treatments enhancing PI3K-Akt signaling reduce disease progression by improving motor function and reducing pathological changes [62]. This enrichment therefore suggests that CNR-401's neuroprotective effects partially operate through activation of survival signaling cascades that counteract BMAA-induced oxidative stress, inflammatory responses, and apoptotic cell death.

For contextual comparison, the BMAA versus control enrichment included terms such as JAK-STAT signaling pathway, P13K-AKT signaling pathway, cytokine-cytokine receptor interaction, and ECM-receptor interaction, confirming that BMAA exposure induces inflammatory and destructive responses characteristic of neurodegenerative injury. The therapeutic enrichment patterns in CNR-401 treatment directly counteract these pathological processes, demonstrating mechanistic specificity in addressing BMAA-induced molecular perturbations.

The convergence of KEGG pathway and GO enrichment analyses establishes that CNR-401's neuroprotective mechanism operates through coordinated modulation of inflammation (cytokine signaling), steroid bioavailability (steroid biosynthesis), antioxidant defense (vitamin metabolism), detoxification (glucuronate and xenobiotic metabolism), and cellular survival (PI3K-Akt)—precisely targeting pathological processes that drive ALS progression.

Comparing to Edaravone and Cannflavin A: Distinct Mechanistic Signatures

The differences between CNR-401's transcriptomic effects and those of Edaravone or Cannflavin A shed light on their divergent mechanisms of action. Edaravone, an FDA-approved ALS drug, is a well-known free radical scavenger that provides neuroprotection by reducing oxidative stress and delaying motor neuron deterioration [63, 1]. Its mechanism operates through direct chemical neutralization of reactive oxygen species, making it fundamentally a non-genomic intervention rather than a transcriptional modulator. In our study, Edaravone treatment after BMAA exposure led to relatively few DEGs (only 359, with the vast majority being downregulations). However, this limited transcriptomic footprint does not align with precise targeting of oxidative stress pathways as the literature claims. Our pathway enrichment analysis revealed no significant enrichment of oxidative stress-related pathways and instead revealed metabolic pathways including steroid biosynthesis, lipid metabolism, and alcohol metabolism, alongside cell signaling pathways such as PI3K-Akt, VEGF, and JAK-STAT signaling (Supplementary Material: Results). This limited yet scattered transcriptomic footprint may explain why Edaravone provides only modest clinical benefits despite FDA approval [1]; The scattered pattern suggests that edaravone lacks the focused potency needed for robust therapeutic intervention. CNR-401, by contrast, alters hundreds of genes across diverse pathways in a more coordinated fashion, suggesting a more comprehensive and effective therapeutic mechanism that addresses multiple aspects of neurodegeneration simultaneously rather than superficially touching many pathways.

Cannflavin A, a flavonoid from Cannabis sativa, was included as another comparator. In our zebrafish ALS model, pure Cannflavin A treatment at 2 μM after BMAA exposure resulted in

130 differentially expressed genes (DEGs), with a predominant upregulation pattern (91 up vs 39 down). Remarkably, the enrichment analysis revealed that Cannflavin A did not significantly enrich inflammatory response pathways, despite its well-established anti-inflammatory properties [13, 14]. Our enrichments showed that it instead activated metabolic, antioxidant, and steroidogenic pathways (Supplementary Material: Results). This apparent discrepancy can be explained by critical pharmacological and mechanistic factors that highlight the complexity of natural product bioactivity translation from *in vitro* to *in vivo* systems. While our 2 µM concentration theoretically exceeds the reported cell-free (*in-vitro*) IC50 values for these enzymes (mPGES-1 inhibition at 1.8 µM and 5-LOX inhibition at 0.9 µM) [13], *in vivo* bioavailability factors, which are known to significantly reduce effective tissue concentrations [64], may have prevented proper inhibition. Critically, Cannflavin A treatment still improved locomotor function in BMAA-exposed zebrafish, demonstrating functional neuroprotective efficacy despite the absence of classical inflammatory pathway modulation. Regardless of through which mechanisms, the scope of changes with Cannflavin A was still limited compared to CNR-401. Notably, Cannflavin A did not trigger the concerted downregulation of UGT enzymes that CNR-401 did, nor did it upregulate DNA repair enzymes or modulate the P13K/Akt pathway, suggesting that these effects are unique to CNR-401. These distinct transcriptomic signatures allow us to directly compare how CNR-401's mechanism differs from these known therapies. Edaravone's signature is one of a scattered modulator with limited effects across diverse pathways and Cannflavin A's signature (at this concentration) was that of a focused modulator of metabolic and steroidogenic functions. CNR-401, however, produced a hybrid signature by combining these elements plus anti-inflammation, regulation of calcium overload, cellular survival through PI3K-Akt signaling, and even DNA-reparative effects.

CNR-401 Has Superior Anti-inflammatory Activity

When CNR-401 was tested at a concentration of 2 µM, the compound demonstrated robust anti-inflammatory gene expression signatures, including significant downregulation of cytokine signaling pathways and *MHC-II* genes (*HLA-DQA1/DQA2*). This anti-inflammatory transcriptomic response is particularly noteworthy given that pure Cannflavin A, when tested at the same 2 µM concentration, failed to enrich canonical inflammatory-response pathways despite its well-established anti-inflammatory properties. The complex botanical composition of CNR-401 may contribute to its broader and more pronounced modulation of inflammatory gene networks through the additive effects of its various components, and potentially through synergistic interactions between them. Although the current study is not designed to assess synergy, such effects have been proposed between cannabinoids and terpenes in various other therapeutic areas [16]. What can be said about these results is that CNR-401 achieves therapeutic anti-inflammatory effects at total concentrations where Cannflavin A would be insufficient, supporting a sophisticated combinatorial strategy that maximizes therapeutic benefit while potentially minimizing the concentration requirements of any single active ingredient.

Future Research Directions

Interpretation of transcriptomic data requires careful consideration as a more extensive change in gene expression (as seen with CNR-401) does not automatically equate to superior clinical efficacy; some changes could be neutral or even maladaptive. The observed *DAO* downregulation in CNR-401-treated subjects exemplifies this complexity. While functional mobility assessments demonstrated that CNR-401 treatment rescues rather than exacerbates BMAA-induced motor deficits, examples like *DAO* emphasize the critical importance of

integrating transcriptomic and functional analyses to accurately evaluate the net therapeutic impact of candidate interventions on disease-relevant outcomes. Although CNR-401 demonstrated a positive net therapeutic effect in this study, the extensive genetic modifications warrant detailed mechanistic investigation to establish clinical relevance for each significant genetic change.

Edaravone's limited transcriptomic signature yet comparable functional outcome seems to suggest that focused molecular interventions can achieve meaningful therapeutic outcomes with minimal transcriptomic disruption. Despite inducing far fewer differentially expressed genes than CNR-401 (359 versus 1,576 DEGs), Edaravone produced comparable functional rescue in our mobility assessments. This indicates that strategic modulation of key pathways may be as effective as broad transcriptomic reprogramming. However, this pattern may simply reflect the limitations of our BMAA-induced ALS model in revealing the full therapeutic potential of CNR-401's multi-pathway modulation. To determine whether CNR-401's extensive genetic changes confer additional therapeutic advantages compared to Edaravone, both compounds should be tested across diverse experimental conditions that challenge different aspects of ALS pathophysiology, such as chronic neurodegenerative models and genetic ALS variants. The potential value of CNR-401's extensive transcriptomic modulation may only become apparent under these specific disease conditions or patient contexts not captured by our current model, emphasizing the critical importance of comprehensive preclinical testing to fully evaluate its therapeutic potential.

Given that the transcript-level changes observed with CNR-401 are now matched by robust functional neuroprotection (the significant rescue of locomotor activity in BMAA-exposed zebrafish), CNR-401 emerges as a promising next-generation multi-target therapeutic candidate for ALS. The convergence of molecular and behavioral efficacy strengthens the rationale for further preclinical development and positions CNR-401 as a lead compound capable of addressing the complex, multifactorial pathology of ALS. Future studies should validate these multi-target genetic interpretations by measuring corresponding biochemical changes, such as neurosteroid levels or oxidative damage markers, in CNR-401-treated subjects. Additionally, comparing CNR-401's transcriptomic signature to those from other ALS models or patient-derived cells could further clarify how this compound fits into the landscape of ALS therapeutics. Nonetheless, the current results are encouraging: they suggest that CNR-401 intervenes in multiple downstream consequences of ALS pathology, potentially offering a broader therapeutic benefit than existing single-mechanism drugs.

CONCLUSIONS

Summary of CNR-401's Neuroprotective Mechanisms

Our transcriptomic analysis reveals that CNR-401 addresses multiple pathological processes underlying ALS through a coordinated molecular response. The compound demonstrates multi-targeted neuroprotection by simultaneously modulating eight key mechanisms:

Neuroinflammation Suppression and ECM Stabilization: CNR-401 downregulates key inflammatory mediators including URGCP and HLA-DQA1/DQA2, while matrix remodeling

gene MXRA5 shows pronounced suppression. GO enrichment reveals terms related to extracellular matrix organization and inflammatory/immune response, while KEGG pathway analysis identifies "cytokine-cytokine receptor interaction" and "ECM-receptor interaction" as significantly enriched, confirming comprehensive modulation of immune signaling networks and ECM stabilization.

Detoxification Pathway Modulation: Coordinated downregulation of 19 human UGT orthologs represents the most striking transcriptomic signature and KEGG pathways "pentose and glucuronate interconversions" and "metabolism of xenobiotics by cytochrome P450" are significantly enriched, indicating fundamental alterations in Phase I and Phase II detoxification processes.

Neurosteroid Biosynthesis Enhancement: The coordinated UGT downregulation directly impacts neurosteroid bioavailability through reduced conjugation, supported by GO and KEGG enrichments of steroid and estrogen metabolic processes. This enhances production and persistence of neuroactive steroids with anti-inflammatory and neuroprotective properties.

Excitotoxicity Modulation: CNR-401's downregulation of DAO likely reflects astrocyte-specific effects or compensatory mechanisms that contribute to CNR-401's comprehensive approach to addressing excitotoxic stress in ALS pathogenesis.

Antioxidant Defense Enhancement: KEGG pathway enrichment reveals "ascorbate and aldarate metabolism" and "retinol metabolism" as significantly enriched pathways, indicating enhanced antioxidant capacity through vitamin C and vitamin A metabolism.

- Regulation of Calcium Overload: GO enrichment of "calcium-mediated signaling" indicates that CNR-401 modulates calcium buffering to prevent calcium overload. This regulation addresses the fundamental "toxic shift" in calcium homeostasis that characterizes motor neuron death.

DNA Repair Enhancement: UNG (Uracil-DNA glycosylase) upregulation indicates enhanced base-excision repair capacity, representing a mechanism not addressed by current ALS therapies. This suggests improved genomic maintenance capacity against oxidative DNA damage.

Cellular Survival Through PI3K-Akt Signaling: KEGG enrichment of "PI3K-Akt signaling pathway" represents a critical finding, as this pathway serves as a central regulator of neuronal survival and neuroprotective mechanisms across neurodegenerative diseases. This suggests CNR-401's effects operate through activation of survival signaling cascades that counteract oxidative stress and apoptotic cell death.

This comprehensive molecular analysis demonstrates that CNR-401's neuroprotective efficacy stems from coordinated multi-pathway modulation rather than single-target effects. Critically, these transcriptomic changes translate into functional neuroprotection, as demonstrated by significant rescue of locomotor deficits in BMAA-exposed zebrafish, confirming that molecular modulation preserves motor outcomes in this ALS model.

ACKNOWLEDGMENTS

The authors thank Ethan Russo, MD for his advice in interpreting the results and Helia Ghazinejad, MBI for assistance with preliminary data analysis.

FUNDING

RNA extraction was funded by the NRC Industrial Research Assistance Program (NRC-IRAP). All other parts of this research were funded by Canurta Therapeutics.

AUTHOR CONTRIBUTIONS

- **K.B., E.S., and A.G.** conceived and designed the experiments.
- **K.B. and E.S.** carried out the experiments.
- **J.C.** provided scientific advisory throughout all steps.
- **I.B. and G.D.** analyzed the data.
- **I.B.** wrote the manuscript.
- All authors read and approved the final manuscript.

DATA AND CODE AVAILABILITY

All data generated and analyzed during this study are provided as in the Supplementary Material which can be found at https://figshare.com/projects/Transcriptomic_Analysis_of_Neuroprotective_Therapies_in_a_Zebrafish_Model_of_ALS/251624. This includes the product toxicity assay results, original normalized RNA-seq data, and the complete set of downstream differential expression data for

all 20 experimental comparisons. Additional figures such as volcano plots, MA plots, heatmaps, and enrichment barplots are also available in the Supplementary Material.

All code for the pipeline used for analysis (the DEG Pipeline Assistant) is available at https://github.com/Shaan7071/DEG-pipeline-assistant. Further information or materials can be requested from the corresponding author.

CONFLICTS OF INTEREST

This research was funded by Canurta Therapeutics, to which the authors belong.

ETHICAL APPROVAL

No formal animal ethics approval was required for this study, as all zebrafish experiments were performed in compliance with relevant institutional and national guidelines for the care and use of laboratory animals.

CONSENT TO PARTICIPATE

Ethics and consent were not required for the performed study.

References

1. Xu, X., Shen, D., Gao, Y., Zhou, Q., Ni, Y., Meng, H., Shi, H., Le, W., Chen, S., & Chen, S. (2021). A perspective on therapies for amyotrophic lateral sclerosis: can disease progression be curbed? Translational Neurodegeneration, 10(1). https://doi.org/https://doi.org/10.1186/s40035-021-00250-5

2. Oliveira, N. A. S., Pinho, B. R., & Oliveira, J. M. A. (2023). Swimming against ALS: How to model disease in zebrafish for pathophysiological and behavioral studies. Neuroscience & Biobehavioral Reviews, 148, 105138. https://doi.org/10.1016/j.neubiorev.2023.105138
3. Banwait, I., & Deol, G. (2025). DEG Pipeline Assistant: An Interactive and Reproducible Pipeline for RNA-seq Differential Expression and Pathway Analysis. Preprint, ResearchHub. https://www.researchhub.com/paper/9398712/deg-pipeline-assistant-an-interactive-and-reproducible-pipeline-for-rna-seq-differential-expression-and-pathway-analysis
4. Newell, M. E., Adhikari, S., & Halden, R. U. (2022). Systematic and state-of-the science review of the role of environmental factors in Amyotrophic Lateral Sclerosis (ALS) or Lou Gehrig's Disease. The Science of the Total Environment, 817, 152504. https://doi.org/10.1016/j.scitotenv.2021.152504
5. Cox, P. A., Banack, S. A., & Murch, S. J. (2003). Biomagnification of cyanobacterial neurotoxins and neurodegenerative disease among the Chamorro people of Guam. Proceedings of the National Academy of Sciences, 100(23), 13380–13383. https://doi.org/https://doi.org/10.1073/pnas.2235808100
6. Lopicic, S., Svirčev, Z., Malešević, T. P., Kopitović, A., Ivanovska, A., & Meriluoto, J. (2022). Environmental Neurotoxin β-N-Methylamino-L-alanine (BMAA) as a Widely Occurring Putative Pathogenic Factor in Neurodegenerative Diseases. Microorganisms, 10(12), 2418. https://doi.org/https://doi.org/10.3390/microorganisms10122418
7. Miyawaki, I. (2020). Application of zebrafish to safety evaluation in drug discovery. Journal of Toxicologic Pathology, 33(4), 197–210. https://doi.org/10.1293/tox.2020-0021

8. Luchtenburg, F. J., Schaaf, M. J. M., & Richardson, M. K. (2019). Functional characterization of the cannabinoid receptors 1 and 2 in zebrafish larvae using behavioral analysis. Psychopharmacology, 236(7), 2049–2058. https://doi.org/10.1007/s00213-019-05193-4
9. Fernández-Ruiz, J., Sagredo, O., Pazos, M. R., García, C., Pertwee, R., Mechoulam, R., & Martínez-Orgado, J. (2013). Cannabidiol for neurodegenerative disorders: important new clinical applications for this phytocannabinoid?. British journal of clinical pharmacology, 75(2), 323–333. https://doi.org/10.1111/j.1365-2125.2012.04341.x
10. Aychman, M. M., Goldman, D. L., & Kaplan, J. S. (2023). Cannabidiol's neuroprotective properties and potential treatment of traumatic brain injuries. Frontiers in Neurology, 14. https://doi.org/10.3389/fneur.2023.1087011
11. Kim, J., Choi, P., Park, Y. T., Kim, T., Ham, J., & Kim, J. C. (2023). The Cannabinoids, CBDA and THCA, Rescue Memory Deficits and Reduce Amyloid-Beta and Tau Pathology in an Alzheimer's Disease-like Mouse Model. International journal of molecular sciences, 24(7), 6827. https://doi.org/10.3390/ijms24076827
12. Del Prado-Audelo, M. L., Cortés, H., Caballero-Florán, I. H., González-Torres, M., Escutia-Guadarrama, L., Bernal-Chávez, S. A., Giraldo-Gomez, D. M., Magaña, J. J., & Leyva-Gómez, G. (2021). Therapeutic Applications of Terpenes on Inflammatory Diseases. Frontiers in pharmacology, 12, 704197. https://doi.org/10.3389/fphar.2021.704197
13. Erridge, S., Mangal, N., Salazar, O., Pacchetti, B., & Sodergren, M. H. (2020). Cannflavins – From plant to patient: A scoping review. Fitoterapia, 146. https://doi.org/https://doi.org/10.1016/j.fitote.2020.104712

14. Barrett, M. L., Gordon, D., & Evans, F. J. (1985). Isolation from cannabis sativa L. of cannflavin—a novel inhibitor of prostaglandin production. Biochemical Pharmacology, 34(11), 2019–2024. https://doi.org/https://doi.org/10.1016/0006-2952(85)90325-9
15. André, R., Gomes, A. P., Pereira-Leite, C., Marques-da-Costa, A., Monteiro Rodrigues, L., Sassano, M., Rijo, P., & Costa, M. D. C. (2024). The Entourage Effect in Cannabis Medicinal Products: A Comprehensive Review. Pharmaceuticals (Basel, Switzerland), 17(11), 1543. https://doi.org/10.3390/ph17111543
16. Russo, E. B. (2011). Taming THC: potential cannabis synergy and phytocannabinoid-terpenoid entourage effects. British Journal of Pharmacology, 163(7), 1344–1364. https://doi.org/https://doi.org/10.1111/j.1476-5381.2011.01238.x
17. Noldus Information Technology. 2023. Daniovision: Automated behavioral tracking system for zebrafish research. Hardware and Software System. Automated tracking system with Etho-Vision XT software.
18. Martin, M. (2011). Cutadapt removes adapter sequences from high-throughput sequencing reads. EMBnet.Journal, 17(1), 10–12.
19. Dobin, A., Davis, C. A., Schlesinger, F., Drenkow, J., Zaleski, C., Jha, S., Batut, P., Chaisson, M., & Gingeras, T. R. (2013). STAR: ultrafast universal RNA-seq aligner. Bioinformatics, 29(1), 15–21. https://doi.org/10.1093/bioinformatics/bts635
20. Dobin, A., & Gingeras, T. R. (2015). Mapping RNA-seq Reads with STAR. Current Protocols in Bioinformatics, 51, 11.14.1-11.14.19. https://doi.org/10.1002/0471250953.bi1114s51
21. Andrews, S. (2010). FastQC: a quality control tool for high throughput sequence data. In Babraham.ac.uk. https://www.bioinformatics.babraham.ac.uk/projects/fastqc/

22. Love, M. I., Huber, W., & Anders, S. (2014). Moderated estimation of fold change and dispersion for RNA-seq data with DESeq2. Genome Biology, 15, 1–21.
23. Son, K., Yu, S., Shin, W., Han, K., & Kang, K. (2018). A Simple Guideline to Assess the Characteristics of RNA-Seq Data. BioMed research international, 2018, 2906292. https://doi.org/10.1155/2018/2906292
24. Rowland, A., Miners, J. O., & Mackenzie, P. I. (2013). The UDP-glucuronosyltransferases: Their role in drug metabolism and detoxification. International Journal of Biochemistry & Cell Biology, 45(6), 1121–1132. https://doi.org/10.1016/j.biocel.2013.02.019
25. Liu, Y., Xi, Y., Chen, G., Wu, X., & He, M. (2020). URG4 mediates cell proliferation and cell cycle in osteosarcoma via GSK3β/β-catenin/cyclin D1 signaling pathway. Journal of Orthopaedic Surgery and Research, 15(1). https://doi.org/https://doi.org/10.1186/s13018-020-01681-y
26. Singh, D. (2022). Astrocytic and microglial cells as the modulators of neuroinflammation in Alzheimer's disease. Journal of Neuroinflammation, 19(1), 206. https://doi.org/https://doi.org/10.1186/s12974-022-02565-0
27. Li, K., Chen, Z., Chang, X., Xue, R., Wang, H., & Guo, W. (2024). Wnt signaling pathway in spinal cord injury: from mechanisms to potential applications. Frontiers in Molecular Neuroscience, 17. https://doi.org/https://doi.org/10.3389/fnmol.2024.1427054
28. Sasabe, J., Miyoshi, Y., Suzuki, M., Mita, M., Konno, R., Matsuoka, M., Hamase, K., & Aiso, S. (2011). D-Amino acid oxidase controls motoneuron degeneration through D-serine. Proceedings of the National Academy of Sciences, 109(2), 627–632. https://doi.org/https://doi.org/10.1073/pnas.1114639109

29. Kondori, N. R., Paul, P., Robbins, J. P., Liu, K., Hildyard, J. C. W., Wells, D. J., & de Belleroche, J. S. (2018). Focus on the Role of D-serine and D-amino Acid Oxidase in Amyotrophic Lateral Sclerosis/Motor Neuron Disease (ALS). Frontiers in Molecular Biosciences, Volume 5-2018. https://doi.org/10.3389/fmolb.2018.00008
30. Youn Lee, J., Young Choi, H., Ahn, H.-J., Gun Ju, B., & Young Yune, T. (2014). Matrix Metalloproteinase-3 Promotes Early Blood–Spinal Cord Barrier Disruption and Hemorrhage and Impairs Long-Term Neurological Recovery after Spinal Cord Injury. The American Journal of Pathology, 184(11), 2985–3000. https://doi.org/https://doi.org/10.1016/j.ajpath.2014.07.016
31. Poveda, J., Sanz, A. B., Fernandez-Fernandez, B., Carrasco, S., Ruiz-Ortega, M., Cannata-Ortiz, P., Ortiz, A., & Sanchez-Niño, M. D. (2017). MXRA5 is a TGF-β1-regulated human protein with anti-inflammatory and anti-fibrotic properties. Journal of Cellular and Molecular Medicine, 21(1), 154–164. https://doi.org/https://doi.org/10.1111/jcmm.12953
32. MedlinePlus Genetics. (2023). HLA-DQA1 gene. U.S. National Library of Medicine. https://medlineplus.gov/genetics/gene/hla-dqa1/
33. Rudy, G. B., & Lew, A. M. (1997). The nonpolymorphic MHC class II isotype, HLA-DQA2, is expressed on the surface of B lymphoblastoid cells. The Journal of Immunology, 158(5), 2116–2125. https://doi.org/https://doi.org/10.4049/jimmunol.158.5.2116
34. Neumann, H., Misgeld, T., Matsumuro, K., & Wekerle, H. (1998). Neurotrophins inhibit major histocompatibility class II inducibility of microglia: Involvement of the p75

neurotrophin receptor. Proceedings of the National Academy of Sciences, 95(10), 5779–5784. https://doi.org/https://doi.org/10.1073/pnas.95.10.5779

35. Schormann, N., Ricciardi, R., & Chattopadhyay, D. (2014). Uracil-DNA glycosylases-Structural and functional perspectives on an essential family of DNA repair enzymes. Protein Science, 23(12), 1667–1685. https://doi.org/https://doi.org/10.1002/pro.2554
36. Chiu, A. S., Gehringer, M. M., Braidy, N., Guillemin, G. J., Welch, J. H., & Neilan, B. A. (2012). Excitotoxic potential of the cyanotoxin β-methyl-amino-l-alanine (BMAA) in primary human neurons. Toxicon, 60(6), 1159–1165. https://doi.org/https://doi.org/10.1016/j.toxicon.2012.07.169
37. Kok, J. R., Palminha, N. M., Dos Santos Souza, C., El-Khamisy, S. F., & Ferraiuolo, L. (2021). DNA damage as a mechanism of neurodegeneration in ALS and a contributor to astrocyte toxicity. Cellular and Molecular Life Sciences, 78(15), 5707–5729. https://doi.org/https://doi.org/10.1007/s00018-021-03872-0
38. Ghorbani, S., & Yong, V. W. (2021). The extracellular matrix as modifier of neuroinflammation and remyelination in multiple sclerosis. Brain, 144(7), 1958–1973. https://doi.org/https://doi.org/10.1093/brain/awab059
39. Maguire, G. (2017). Amyotrophic lateral sclerosis as a protein level, non-genomic disease: Therapy with S2RM exosome released molecules. World Journal of Stem Cells, 9(11), 187–202. https://doi.org/https://doi.org/10.4252/wjsc.v9.i11.187
40. Komine, O., & Yamanaka, K. (2015). Neuroinflammation in motor neuron disease. Nagoya Journal of Medical Science, 77(4), 537–549. https://pmc.ncbi.nlm.nih.gov/articles/PMC4664586/#sec13

41. Liu, Jia, & Wang, F. (2017). Role of Neuroinflammation in Amyotrophic Lateral Sclerosis: Cellular Mechanisms and Therapeutic Implications. Frontiers in Immunology, 8(1005). https://doi.org/https://doi.org/10.3389/fimmu.2017.01005

42. Leal, S. S., & Gomes, C. M. (2015). Calcium dysregulation links ALS defective proteins and motor neuron selective vulnerability. Frontiers in Cellular Neuroscience, 9. https://doi.org/https://doi.org/10.3389/fncel.2015.00225

43. Grosskreutz, J., Van Den Bosch, L., & Keller, B. U. (2010). Calcium dysregulation in amyotrophic lateral sclerosis. Cell Calcium, 47(2), 165–174. https://doi.org/https://doi.org/10.1016/j.ceca.2009.12.002

44. Guatteo, E., Carunchio, I., Pieri, M., Albo, F., Canu, N., Mercuri, N. B., & Zona, C. (2007). Altered calcium homeostasis in motor neurons following AMPA receptor but not voltage-dependent calcium channels' activation in a genetic model of amyotrophic lateral sclerosis. Neurobiology of Disease, 28(1), 90–100. https://doi.org/https://doi.org/10.1016/j.nbd.2007.07.002

45. Garcia-Segura, L. M., & Balthazart, J. (2009). Steroids and neuroprotection: New advances. Frontiers in Neuroendocrinology, 30(2), 5–9. https://doi.org/https://doi.org/10.1016/j.yfrne.2009.04.006

46. Borowicz, K. K., Piskorska, B., Banach, M., & Czuczwar, S. J. (2011). Neuroprotective Actions of Neurosteroids. Frontiers in Endocrinology, 2. https://doi.org/https://doi.org/10.3389/fendo.2011.00050

47. Puig-Bosch, X., Ballmann, M., Bieletzki, S., Antkowiak, B., Rudolph, U., Zeilhofer, H. U., & Rammes, G. (2023). Neurosteroids Mediate Neuroprotection in an In Vitro Model of Hypoxic/Hypoglycaemic Excitotoxicity via δ-GABAA Receptors without Affecting

Synaptic Plasticity. International Journal of Molecular Sciences, 24(10). https://doi.org/https://doi.org/10.3390/ijms24109056

48. Brann, D. W., Dhandapani, K., Wakade, C., Mahesh, V. B., & Khan, M. M. (2007). Neurotrophic and neuroprotective actions of estrogen: Basic mechanisms and clinical implications. Steroids, 72(5), 381–405. https://doi.org/https://doi.org/10.1016/j.steroids.2007.02.003

49. Bustamante-Barrientos, F. A., Méndez-Ruette, M., Ortloff, A., Luz-Crawford, P., Rivera, F. J., Figueroa, C. D., Molina, L., & Bátiz, L. F. (2021). The Impact of Estrogen and Estrogen-Like Molecules in Neurogenesis and Neurodegeneration: Beneficial or Harmful? Frontiers in Cellular Neuroscience, 15. https://doi.org/https://doi.org/10.3389/fncel.2021.636176

50. Cardona-Rossinyol, A., Mir, M., Caraballo-Miralles, V., Lladó, J., & Olmos, G. (2013). Neuroprotective Effects of Estradiol on Motoneurons in a Model of Rat Spinal Cord Embryonic Explants. Cellular and Molecular Neurobiology, 33(3), 421–432. https://doi.org/https://doi.org/10.1007/s10571-013-9908-9

51. Chen, J., Hu, R., Ge, H., Duanmu, W., Li, Y., Xue, X., Hu, S., & Feng, H. (2015). G-protein-coupled receptor 30-mediated antiapoptotic effect of estrogen on spinal motor neurons following injury and its underlying mechanisms. Molecular Medicine Reports, 12(2), 1733–1740. https://doi.org/https://doi.org/10.3892/mmr.2015.3601

52. Munteanu, C., Galaction, A. I., Turnea, M., Blendea, C. D., Rotariu, M., & Poștaru, M. (2024). Redox Homeostasis, Gut Microbiota, and Epigenetics in Neurodegenerative Diseases: A Systematic Review. Antioxidants, 13(9). https://doi.org/https://doi.org/10.3390/antiox13091062

53. Rice, M. E. (2000). Ascorbate regulation and its neuroprotective role in the brain. Trends in Neurosciences, 23(5), 209–216. https://doi.org/https://doi.org/10.1016/s0166-2236(99)01543-x

54. Plascencia-Villa, G., & Perry, G. (2023). Roles of Oxidative Stress in Synaptic Dysfunction and Neuronal Cell Death in Alzheimer's Disease. Antioxidants, 12(8). https://doi.org/https://doi.org/10.3390/antiox12081628

55. Petrovic, S., Arsic, A., Ristic-Medic, D., Cvetkovic, Z., & Vucic, V. (2020). Lipid Peroxidation and Antioxidant Supplementation in Neurodegenerative Diseases: A Review of Human Studies. Antioxidants, 9(11). https://doi.org/https://doi.org/10.3390/antiox9111128

56. Yan, Y., Zhang, A., Dong, H., Ge, Y., Sun, H., Wu, X., Han, Y., & Wang, X. (2017). Toxicity and detoxification effects of herbal Caowu via ultra performance liquid chromatography/mass spectrometry metabolomics analyzed using pattern recognition method. Pharmacognosy Magazine, 13(52), 683–692. https://doi.org/https://doi.org/10.4103/pm.pm_475_16

57. Sun, H., Zhang, A., Song, Q., Fang, H., Liu, X., Su, J., Yang, L., Yu, M., & Wang, X. (2018). Functional metabolomics discover pentose and glucuronate interconversion pathways as promising targets for Yang Huang syndrome treatment with Yinchenhao Tang. RSC Advances, 8(64), 36831–36839. https://doi.org/https://doi.org/10.1039/c8ra06553e

58. Snyder, M. J. (2000). Cytochrome P450 enzymes in aquatic invertebrates: recent advances and future directions. Aquatic Toxicology, 48(4), 529–547. https://doi.org/https://doi.org/10.1016/s0166-445x(00)00085-0

59. Liu, Jun, Zhang, D., Zhang, L., Wang, Z., & Shen, J. (2022). New Insight on Vitality Differences for the Penaeid Shrimp, Fenneropenaeus chinensis, in Low Salinity Environment Through Transcriptomics. Frontiers in Ecology and Evolution, 10. https://doi.org/https://doi.org/10.3389/fevo.2022.716018

60. Rai, S. N., Dilnashin, H., Birla, H., Singh, S. S., Zahra, W., Rathore, A. S., Singh, B. K., & Singh, S. P. (2019). The Role of PI3K/Akt and ERK in Neurodegenerative Disorders. Neurotoxicity Research, 35, 775–795. https://doi.org/https://doi.org/10.1007/s12640-019-0003-y

61. Chen, Y., Hsu, C., Chen, X., Zhang, H., & Peng, W. (2023). Editorial: Regulation of PI3K/Akt signaling pathway: A feasible approach for natural neuroprotective agents to treat various neuron injury-related diseases. Frontiers in Pharmacology, 14(1134989). https://doi.org/https://doi.org/10.3389/fphar.2023.1134989

62. Qi, Y., Yang, C., Zhao, H., Deng, Z., Xu, J., Liang, W., Sun, Z., & Dirk, J. (2022). Neuroprotective Effect of Sonic Hedgehog Mediated PI3K/AKT Pathway in Amyotrophic Lateral Sclerosis Model Mice. Molecular Neurobiology, 59, 6971–6982. https://doi.org/https://doi.org/10.1007/s12035-022-03013-z

63. Singh, P., Belliveau, P., Towle, J., Neculau, A. E., & Dima, L. (2024). Edaravone Oral Suspension: A Neuroprotective Agent to Treat Amyotrophic Lateral Sclerosis. American Journal of Therapeutics, 31(3), 258–267. https://doi.org/https://doi.org/10.1097/MJT.0000000000001742

64. Stielow, M., Witczyńska, A., Kubryń, N., Fijałkowski, Ł., Nowaczyk, J., & Nowaczyk, A. (2023). The Bioavailability of Drugs—The Current State of Knowledge. Molecules, 28(24), 8038. https://doi.org/https://doi.org/10.3390/molecules28248038